CHAPTER 2

Synthesis and characterization of bioactive ligands.

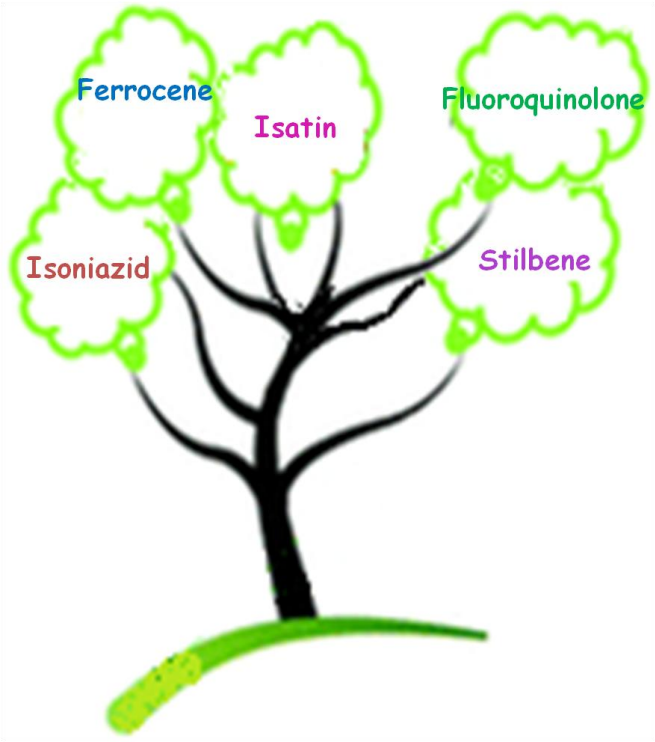

This chapter focuses on the synthesis and characterization of a selected range of five different organic compound series whose bioactivities are well established and can fetch hetero-atoms (N,O) as coordination sites to the ruthenium (II) centre in order to design good biologically active metal complexes with an aim to study their potential as anticancer agents. These ligands have been synthesized and well characterized by Mass spectrometry, NMR, FTIR and UV-Vis spectroscopy. Except for the stilbene derivatives (monodentate) all other ligands are bidentate.

Section 2.2 of this chapter is based on the article: Pulipaka Ramadevi, Rinky Singh, Akhilesh Prajapati, Sarita Gupta, Debjani Chakraborty* *Advances in Chemistry*, **2014**, doi: 10.1155/2014/630575.

Section 2.3 of this chapter is based on the article: Pulipaka Ramadevi, Rinky Singh, Sarmita S Jana, Ranjitsinh Devkar, Debjani Chakraborty* *Journal of Photochemistry and Photobiology A: Chemistry*, **2015**, *305*, 1-10.

TABLE OF CONTENTS

2.1 Biological and medicinal importance of Heterocyclic compounds:

Compounds containing N, S and O as hetero atoms (heterocyclic compounds) form by far the largest of classical divisions of organic chemistry and are of immense importance biologically and industrially. The majority of pharmaceuticals and biologically active agrochemicals are heterocyclic while countless additives and modifiers used in industrial applications ranging from cosmetics, reprography information storage and plastics are heterocyclic in nature. One striking structural features inherent to heterocycles, which continue to be exploited to great advantage by the drug industry, lies in their ability to manifest substituents around a core scaffold in defined three dimensional representations. They have contributed to the development of society from a biological and industrial point of view as well as to the understanding of life processes and to the efforts to improve the quality of life. Many natural drugs [1-4] such as papaverine, theobromine, quinine, emetine, theophylline, atropine, procaine, codeine, reserpine and morphine are heterocycles. Almost all the compounds we know as synthetic drugs such as diazepam, chlorpromazine, isoniazid, fluoroquinolones, metronidazole, azidothymidine, barbiturates, antipyrine, captopril and methotrexate are also heterocycles. All these natural and synthetic heterocyclic compounds can and do participate in chemical reactions in the human body. Many fundamental manifestations of life as the provision of energy, transmission of nerve impulses, sight, metabolism and the transfer of hereditary information are all based on chemical reactions involving the participation of many heterocyclic compounds, such as vitamins, enzymes, coenzymes, nucleic acids, ATP and serotonin [5]. Why does nature utilize heterocycles? The answer to this question is provided by the fact that heterocyles are able to get involved in an extraordinarily wide range of reaction types. Depending on the pH of the medium, they may behave as acids or bases, forming anions or cations. Some interact readily with electrophilic reagents, others with nucleophiles, yet others with both. Some are easily oxidized, but resist reduction, while others can be readily hydrogenated but are stable toward the action of oxidizing agents. Certain amphoteric heterocyclic systems simultaneously demonstrate all of the above-mentioned properties. The ability of many heterocycles to produce stable complexes with metal ions has great biochemical significance. The presence of different heteroatoms makes tautomerism ubiquitous in the heterocyclic series. Such versatile reactivity is linked to the electronic distributions in heterocyclic molecules. Moreover such electronic properties of heterocyclic compounds make them good metal chelators (donor ligands).

Synthetic heterocycles have widespread therapeutic uses such as antibacterial, antifungal, antimycobacterial, trypanocidal, anti-HIV activity, antileishmanial agents, genotoxic, antitubercular, antimalarial, herbicidal, analgesic, antiinflammatory, muscle relaxants,

anticonvulsant, anticancer and lipid peroxidation inhibitor, hypnotics, antidepressant, antitumoral, anthelmintic and insecticidal agents [6-11].

In conclusion, it can be questioned why it is specifically appropriate to emphasize the role of heterocycles. Introduction of a heteroatom into a cyclic compound imparts new properties. Heterocycles are chemically more flexible and better able to respond to the many demands of biochemical systems. It is known that existence of metal ions bonded to such biologically active heterocyclic compounds may enhance their activities.

With this view point the work in this chapter encases the synthesis of five different systems containing heterocycles as well as free hetero atoms, with well established biological activities.

2.2 Isoniazid (INH) Schiff bases

2.2.1 Introduction:

INH is a first generation anti-tubercular drug that keeps an analogy with isonicotinic acid, an isomer of nicotinic acid (*Fig.2.1*). Nicotinic acid, also known as vitamin B3 and niacin, as well as its amide niacinamide are found in several aliments and animals, and play an important role in different biological processes [12]. This class of heterocyclic compounds also show a broad spectrum of biological activities, such as anti-carcinogenic [13], antioxidant [14], anti-inflammatory [15], and anti-bacterial [16]. INH displays a critical role in the initial phase of tuberculosis (TB) therapy [17] and the most accepted mechanism of action for INH involves the inhibition of biosynthesis of mycolic acids, a class of compounds found in the cell wall of the *M. tuberculosis* [18]. However, in spite of the relevance of isoniazid in tuberculosis treatment in the last twenty years, this drug has rarely been studied in the field of cancer [19], even after promising perspectives of analogues of isoniazid in this field, which can be illustrated by the work of Malhotra and co-workers, wherein they synthesized isonicotinoyl hydrazones by condensing isoniazid with various aldehydes, acetophenones and benzophenones and these were evaluated for their anti-cancer activity against lung, colon, CNS, ovarian, renal and prostrate cancer. All the synthesized compounds displayed moderate to potent anticancer activity of which the fluoro and nitro derivatives showed the highest potency. Derivatization of INH, particularly into Schiff bases (isonicotinoyl hydrazones), increases the lipophilitcity of INH resulting into enhancement of absorption through biomembranes making the drug more readily available for its action [20]. Their potency as anticancer agent is reflected from the little work that has been published so far where in a few researchers have synthesized hydrazones of INH and their iron complexes and evaluated them for their

antitumoral activity suggesting a mechanism of inhibition of ribonucleotide reductase [21].

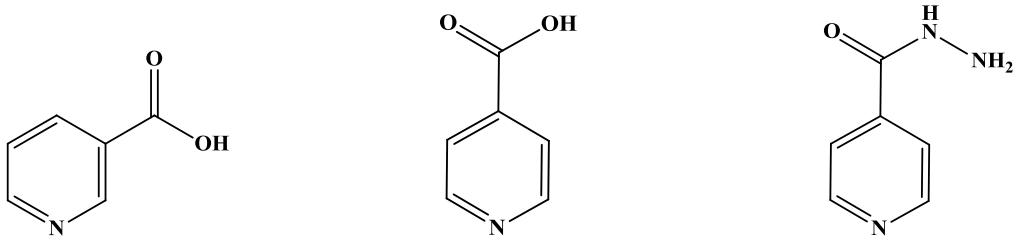

A **B** **C**

Fig.2.1: *Structures of (**A**) Nicotinic acid, (**B**) Isonicotinic acid and (**C**) Isoniazid respectively.*

Here a series of four isonicotinoyl hydrazones have been synthesized employing four different aromatic aldehydes.

2.2.2 Materials and instrumentation:

All the chemicals and solvents used for the synthesis and characterization of ligands are of analytical grade and were used as purchased. INH (isonicotinoyl hydrazine) was purchased from Acros organics and the aldehydes were purchased from SRL (Sisco research laboratory, Mumbai, India.).

^{1}H and ^{13}C NMR spectra were recorded on Bruker 400 MHz NMR Spectrophotometer. Mass spectra of the ligands were recorded on Thermoscientific DSQ – II Mass spectrometer. Infrared spectra (400-4000cm^{-1}) were recorded on Perkin Elmer RX-1 FTIR with samples prepared as KBr pellets. UV spectra were recorded in DMSO solution at concentrations around 10^{-3}M on Perkin Elmer Lambda-35 dual beam UV-Vis spectrophotometer.

2.2.3 Synthesis and characterization:

INH, aldehyde and $NiCl_2.6H_2O$ were taken in the mole ratio of 1:1:0.5 in 20 ml dry methanol, few drops of acetic acid was added to adjust the pH to 5 and refluxed for 1-2 h. The product obtained was filtered and recrystallized from absolute ethanol. *Fig. 2.2* shows the general scheme for the synthesis of isoniazid Schiff's bases **Inh 1-4**.

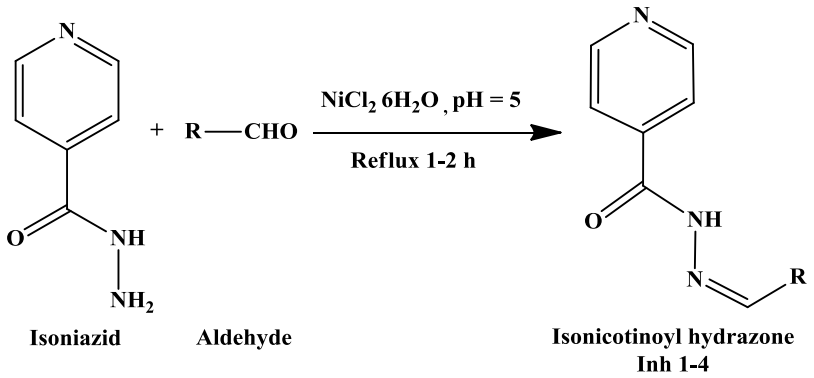

Fig. 2.2: *General synthetic scheme for the synthesis of Isoniazid Schiff bases.*

(N'-benzylideneisonicotinohydrazide) (**Inh-1**)

Inh-1 was prepared by condensation of isoniazid (3.6 mmol, 500 mg) and benzaldehyde (3.6 mmol, 386 mg) in presence of $NiCl_2.6H_2O$ (1.8 mmol, 433 mg). Pale yellow crystals were obtained. Solubility: DMSO, DMF; Yield 84.14%, mp 197°C; Molecular Weight 225.25 g/mol; Molecular Formula $C_{13}H_{11}N_3O$; MS *m/z*: 225.09 (M^+); δ_H (400 MHz, DMSO-d_6) 12.10 (s, 1H, NH), 8.79 (d, *J* 5.2, 2H, pyridyl α-H), 8.47 (s, 1H, N=CH), 7.83 (d, *J* 4.4, 2H, pyridyl β-H), 7.77-7.75 (dd, J_1 7.6, J_2 2, 2H, Ar-H), 7.51-7.47 (m, 3H, Ar-H); δ_C (400 MHz, DMSO-d_6) 162.1, 150.8, 149.4, 140.9, 134.4, 130.8, 129.3, 127.7, 122.0; FTIR (KBr)/cm^{-1} $\nu_{C=N}$ 1598(s), ν_{N-H} 3197(b), $\nu_{C=O}$ 1694(s).

(N'-(2-hydroxybenzylidene)isonicotinohydrazide) (**Inh-2)**

Inh-2 was prepared by condensation of isoniazid (3.6 mmol, 500 mg) and salicylaldehyde (3.6 mmol, 445 mg) in presence of $NiCl_2.6H_2O$ (1.8 mmol, 433 mg). Yellow crystals were obtained. Solubility: DMSO, DMF; Yield 87.2%; mp 248°C; Molecular Weight 241.25 g/mol; Molecular Formula $C_{13}H_{11}N_3O_2$; MS *m/z*: 241.07 (M^+); δ_H (400 MHz, DMSO-d_6) 12.31 (s, 1H, NH), 11.08 (s, 1H, OH), 8.80 (d, *J* 4.4, 2H, pyridyl α-H), 8.68 (s, 1H, N=CH), 7.85 (d, *J* 4.4, 2H, pyridyl β-H), 7.62-7.60 (dd, J_1 7.6, J_2 1.6, 1H, Ar-H), 7.34-7.29 (t, *J* 8.4, 1H, Ar-H), 6.95-6.91 (m, 2H, Ar-H); δ_C (400 MHz, DMSO-d_6) 161.7, 157.9, 150.8, 149.3, 140.4, 132.2, 129.6, 121.9, 119.8, 119.1, 116.9; FTIR (KBr)/cm^{-1} $\nu_{C=N}$ 1613(s), ν_{N-H} 3179(b), $\nu_{C=O}$ 1679(s).

(N'-(4-hydroxy-3-methoxybenzylidene)-N-methylisonicotinohydrazide) (**Inh-3**)

Inh-3 was prepared by condensation of isoniazid (3.6 mmol, 500 mg) and vanillin (3.6 mmol, 554 mg) in presence of $NiCl_2.6H_2O$ (1.8 mmol, 433 mg). Yellowish brown crystals were obtained. Solubility: DMSO, DMF; Yield 79.06%; mp 226°C; Molecular Weight

271.27 g/mol; Molecular Formula $C_{14}H_{13}N_3O_3$; MS *m/z*: 271.09 (M^+); δ_H (400 MHz, DMSO-d_6) 11.91 (s, 1H, NH), 9.65 (s, 1H, OH), 8.78 (d, *J* 5.2, 2H, pyridyl α-H), 8.35 (s, 1H, N=CH), 7.81 (d, *J* 6.0, 2H, pyridyl β-H), 7.33 (d, *J* 1.2, 1H, Ar-H), 7.13–7.10 (dd, J_1 8.0, J_2 1.6, 1H, Ar-H), 6.85 (d, *J* 8, 1H, Ar-H), 3.83 (s, 3H, OCH_3); δ_C (400 MHz, DMSO-d_6) 161.8, 150.7, 150.0, 149.7, 148.5, 141.1, 125.8, 122.9, 121.9, 115.9, 109.4, 55.9; FTIR (KBr)/cm^{-1} $\nu_{C=N}$ 1595(s), ν_{N-H} 3231(b), $\nu_{C=O}$ 1649(s), ν_{O-H} 3416(b).

(N'-(4-methoxybenzylidene)-N-methylisonicotinohydrazide) (**Inh-4**)

Inh-4 was prepared by condensation of isoniazide (3.6 mmol, 500 mg) and p-anisaldehyde (3.6 mmol, 495 mg) in presence of $NiCl_2.6H_2O$ (1.8 mmol, 433 mg). Pale yellow crystals were obtained. Solubility: DMSO, DMF; Yield 89.37%; mp 138°C; Molecular Weight 255.27 g/mol; Molecular Formula $C_{14}H_{13}N_3O_2$; MS *m/z*: 255.09 (M^+); δ_H (400 MHz, DMSO-d_6) 11.96 (s, 1H, NH), 8.78 (d, *J* 4.4, 2H, pyridyl α-H), 8.40 (s, 1H, N=CH), 7.82 (d, *J* 4.4, 2H, pyridyl β-H), 7.70 (d, *J* 8.8, 2H, Ar-H), 7.03 (d, *J* 6.8, 2H, Ar-H), 3.81 (s, 3H, OCH_3); δ_C (400 MHz, DMSO-d_6) 161.8, 161.5, 150.7, 149.3, 141.0, 129.3, 126.9, 121.9, 114.8, 55.7; FTIR (KBr)/cm^{-1} $\nu_{C=N}$ 1611(s), ν_{N-H} 3242(b), $\nu_{C=O}$ 1662(s).

2.2.4 Results and discussion:

In a general sense, transition metal-based catalyzed reactions can be viewed as template reactions where reactants coordinate to adjacent sites on the metal ion and, owing to their adjacency, the two reactants interconnect (insert or couple) either directly or via the action of another reagent. Template effects may arise from stereochemistry imposed by metal ion coordination of some of the reactants, promoting a series of controlled steps and characteristically provides routes to products not formed in the absence of the metal ion. Appreciable amount of work has been done on one pot multi-component synthesis of Schiff bases using transition metal ions as templates [22]. Following this insight we carried out the Ni(II) mediated Schiff base synthesis and found that the reaction time had reduced and product yields had increased markedly.

The composition and structures of all the four hydrazones have been confirmed by ^1H and ^{13}C NMR, mass spectrometry, infrared spectroscopy and UV-Vis spectroscopy. The analytical data are consistent with the proposed structures and their empirical formulas.

The IR spectra of ligands **Inh 1-4** typically show strong secondary amide carbonyl absorption at 1650-1700 cm^{-1}. In all the ligands, the $\nu_{C=N}$ band is obtained between 1600-1613 cm^{-1}. The free N-H stretching bands are found in the range of 3150-3250 cm^{-1}.

The UV spectra show bands in the wavelength range 200-350 nm. The first band appearing within 210-225 nm region can be assigned to the π→π* transition of the aromatic rings (*Fig. 2.3*). The second band observed within 280-330 nm region is due to the excitation of the electrons of the azomethine group which corresponds to an intra-ligand *n*→π* transition [23]. In case of **Inh-2** there is a third band located at 328 nm that can be ascribed to charge transfer within the entire Schiff base molecule. This band is commonly observed in *o*-hydroxyl Schiff bases [24] and is based on strong intramolecular hydrogen bonding between the hydroxyl group of the salicylidene and the azomethine nitrogen [25]. The peak values have been tabulated in *Table 2.1*.

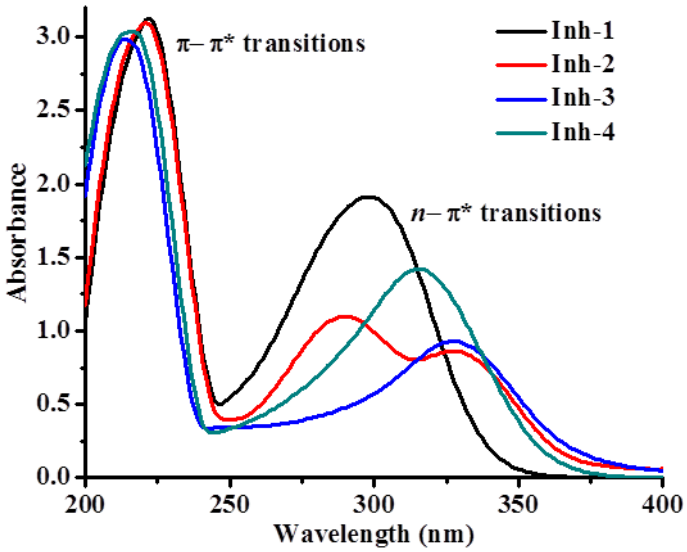

Fig. 2.3: *UV spectra of ligands* ***Inh 1-4*** *recorded in DMSO with path length 1 cm.*

Table 2.1: *UV peak assignments of* ***Inh 1-4***

Compound	***Intra-ligand Transitions (nm)***	
	π-π*	***n-π****
Inh-1	222	298
Inh-2	221	289, 328
Inh-3	214	327
Inh-4	216	316

The mass spectra of ligands **Inh 1-4** show peaks corresponding to the molecular ions M^+ at *m/z* = 225.09, 241.07, 271.09 and 255.09 respectively (*Fig. 2.4*). In addition the mass spectra of all the ligands show prominent peaks at *m/z* = 106 and 78 corresponding to (pyridin-4-ylmethylidyne)oxonium and pyridin-4-ylium fragments respectively.

The ^{1}H NMR spectra of the ligands **Inh 1-4** (*Fig.2.5**)** are in well agreement with their proposed structures. The N-H proton of the diazenyl group (N=NH) shows a one proton singlet at a δ value of 12 ppm and the imine proton N=CH shows a one proton singlet at a δ value 8.4-8.7 ppm confirming the condensation of isoniazid with aryl aldehydes. Rest of the signals can be attributed to the aromatic protons of the pyridyl ring of isoniazid and the aryl substitution on the aldehyde group.

The ^{13}C NMR spectra of **Inh 1-4** (*Fig. 2.6*) show prominent peaks at δ = 149, 122 and 134 ppm for pyridyl α, β and γ carbon respectively with respect to pyridyl N. All the ligands show peak for azomethine carbon at δ ~ 150.8 ppm and carbonyl carbon at δ ~ 161 ppm confirming the hydrazone formation between the aldehydes and isoniazid. The peak at 157 ppm in **Inh-2** is attributable to the aryl carbon carrying the hydroxyl group whereas peak at ~ 55 ppm in both **Inh-3** and **4** is owing to methoxy carbon.

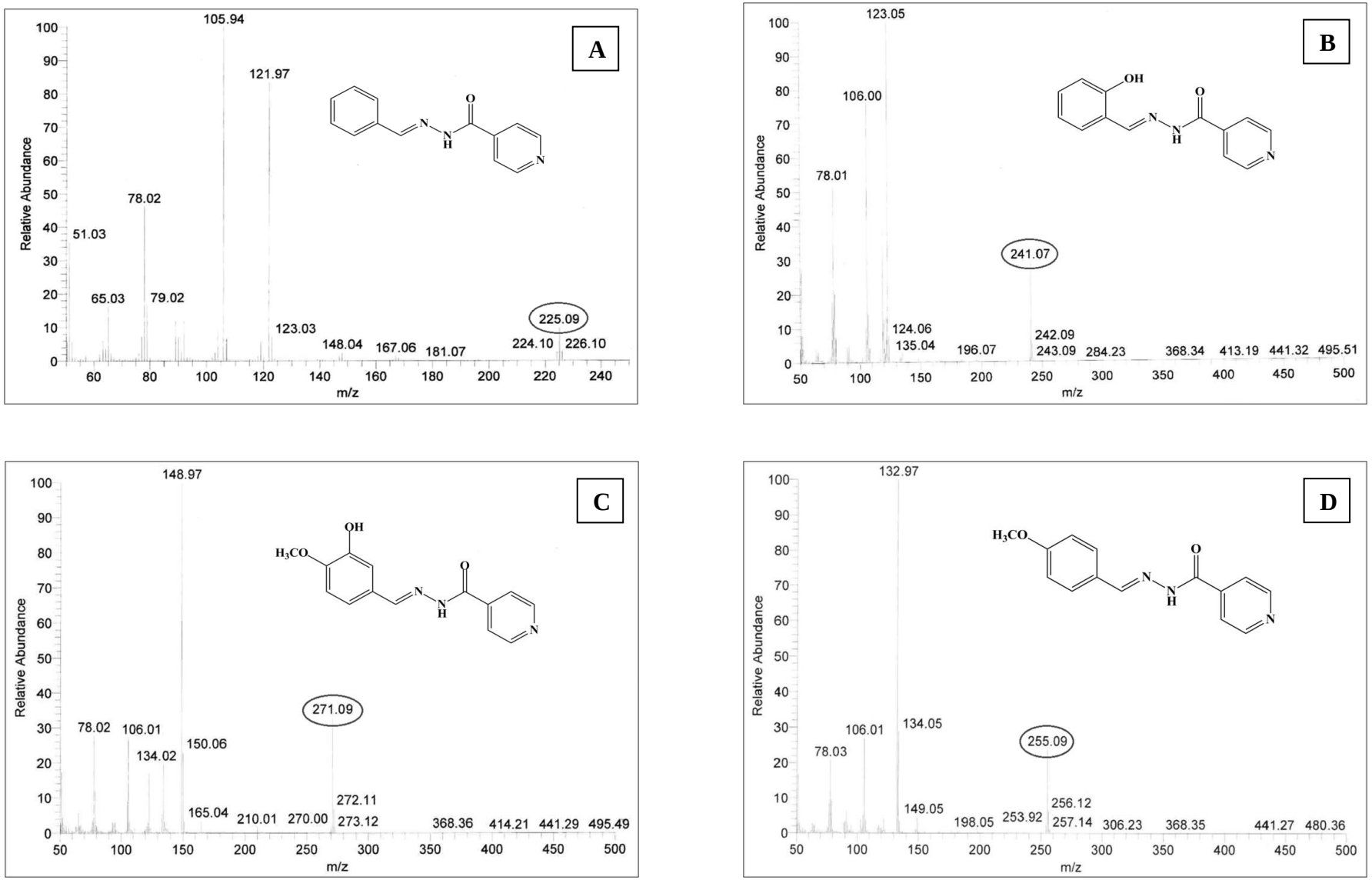

Fig. 2.4: *Mass spectra of ligands (A)* ***Inh-1*** *(B)* ***Inh-2*** *(C)* ***Inh-3*** *(D)* ***Inh-4*** *indicating the molecular ion peak.*

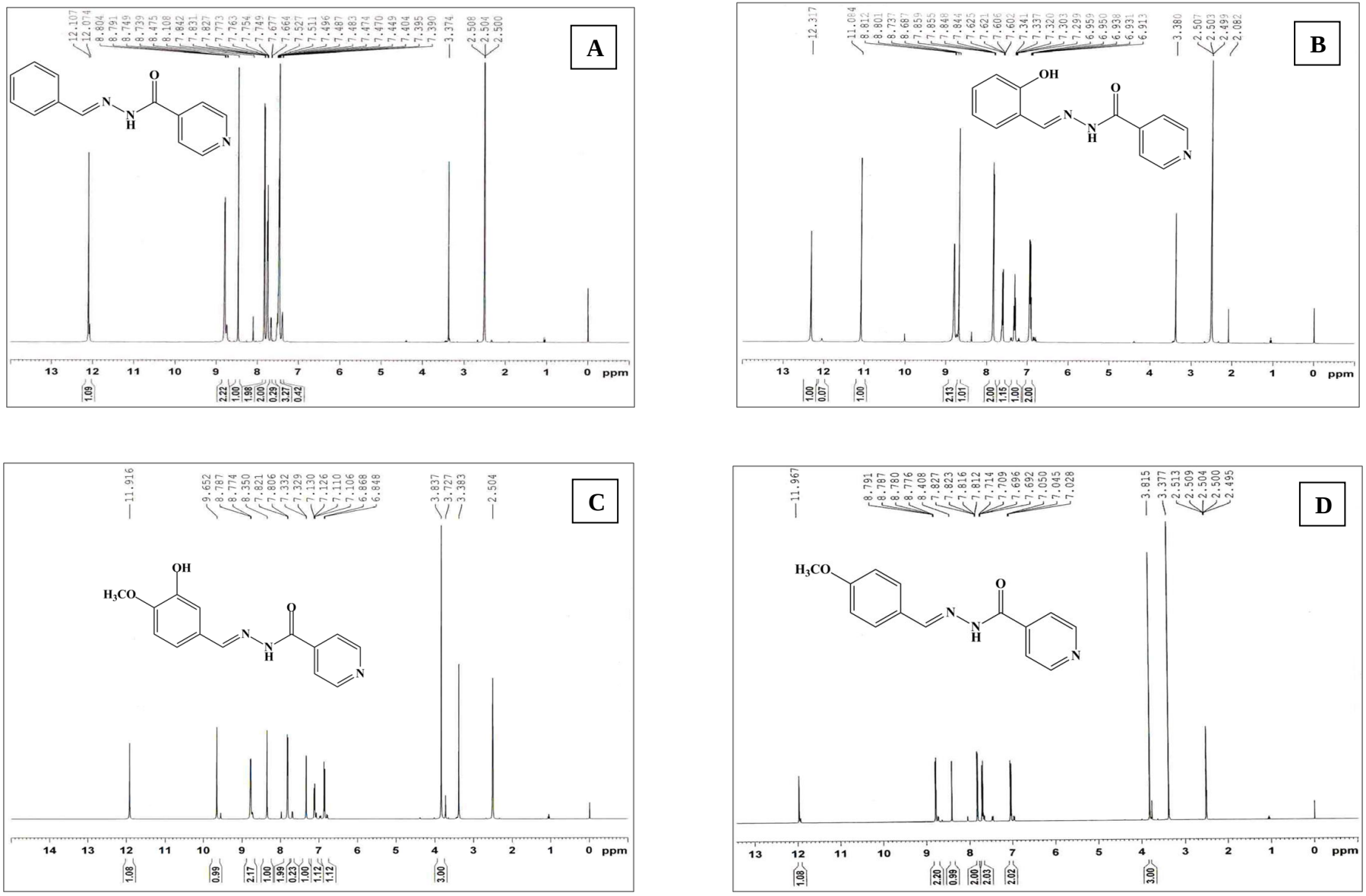

Fig. 2.5: *^{1}H NMR spectra of ligands (A)* ***Inh-1*** *(B)* ***Inh-2*** *(C)* ***Inh-3*** *(D)* ***Inh-4***

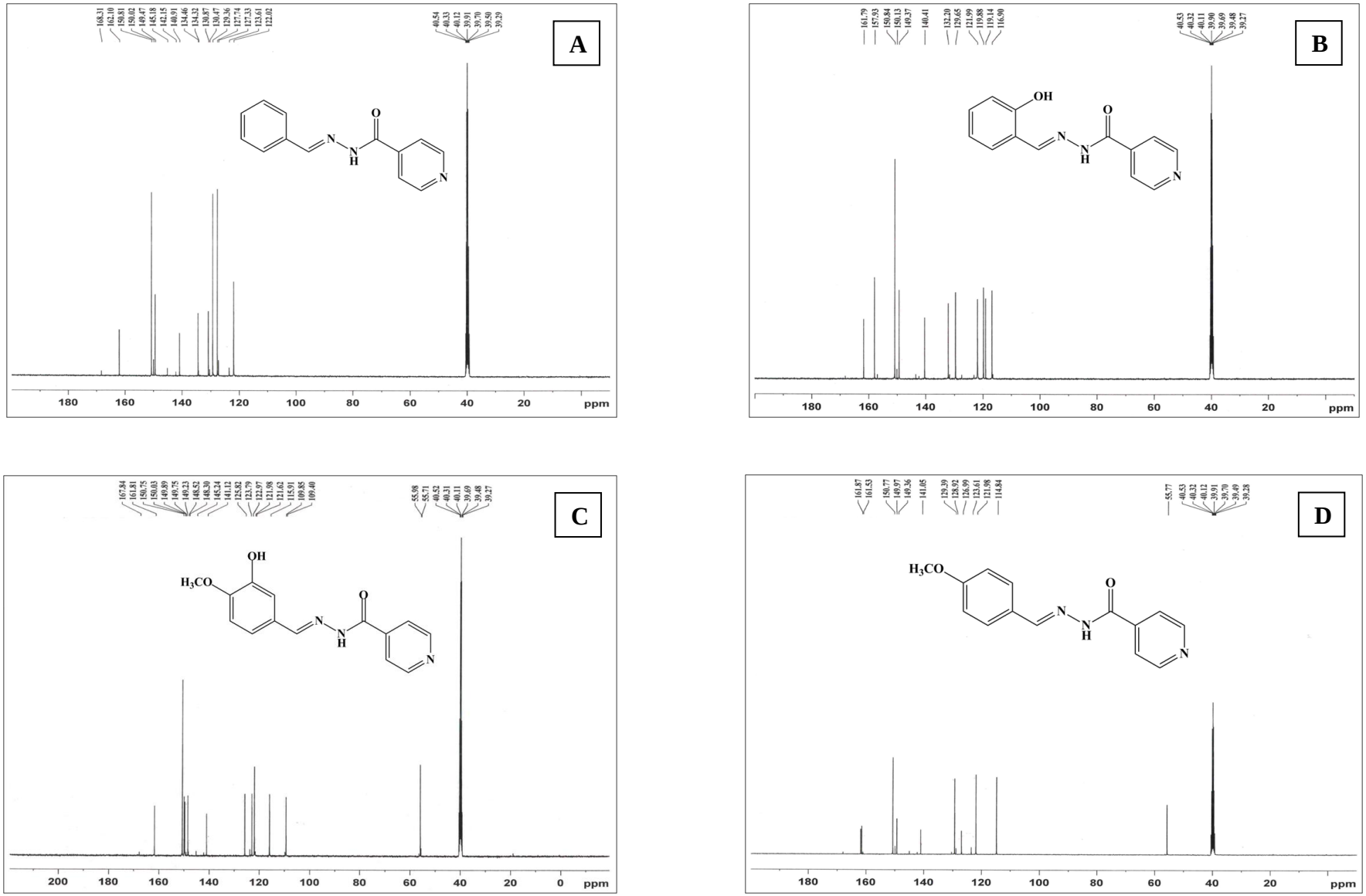

Fig. 2.6: *^{13}C NMR spectra of ligands (A)* ***Inh-1*** *(B)* ***Inh-2*** *(C)* ***Inh-3*** *(D)* ***Inh-4***

2.3 Ferrocene Mannich bases

2.3.1 Introduction:

Ferrocene is one of the members of the well known organometallic family- "metallocenes" in which an iron atom is flanked by two cyclopentadienyl (Cp) rings. The unique structural and conformational properties of ferrocene, an atomic ball bearing character, are characterized by the parallel alignment of the two cyclopentadienyl rings and the free rotation of the rings around the axis penetrating their centers. Its remarkable stability and fascinating chemistry has attracted the attention of the scientific and technical community. Owing to the favourable electronic properties of ferrocene and its easy functionalization their applications have been explored in a wide range of scientific areas ranging from catalysis to the design of new nonlinear optic materials to new biologically active compounds. Several structural modifications of established drugs with ferrocenyl moiety have been reported, such as ferrocene fluconazole [26], ferrocene aspirin [27], mefloquine [28] and artemisinin [29]. Moreover ferrocene derivatives have been used as scaffolds to design new molecules that recognize cations, anions, organic molecules, nucleobases, dinucleotides and amino acids [30-35]. Mitsuo Sekine *et al* [36] have reported new DNA binding molecules utilizing structural and conformational properties of ferrocene. Their design concept is based on the fact that the distance between the two cyclopentadienyl rings of ferrocene, ca. 3.3 Å is close to the distance between two aromatic rings stacked with each other. In addition, it is well-known that the minor groove of DNA can accommodate stacked aromatic rings, as established by the structural studies of natural or synthetic molecules that recognize the minor groove. Therefore, it was expected that ferrocene derivatives could be a new type of DNA binding molecules if appropriately designed aromatic rings were attached to the Cp rings. The stability of ferrocene in aqueous and aerobic media has made ferrocenyl compounds very popular molecules for such biological applications. Furthermore such favorable characteristics of ferrocene led to the design of ferrocenyl derivatives that function as highly sensitive detectors of proteins or as reporters of protein activity. Recent studies on ferrocenyl conjugates with amino acids and end-labeled ferrocenyl di- and tripeptides have demonstrated distinctive electrical, structural, and medicinal properties [37].

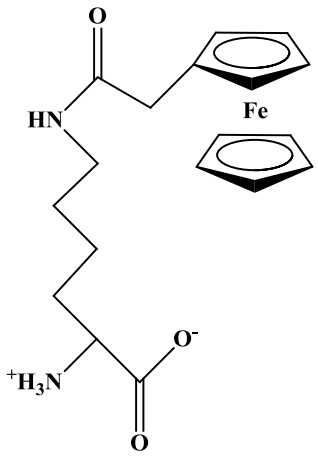

Fig. 2.7: *Unnatural amino acid* N^{α}-N^{ε}*-(ferrocene-1-acetyl)-L-lysine: A novel organometallic nuclease*

Many researchers have shown interest in design of unnatural ferrocenyl amino acids and peptides which further have been studied for their biomedical applications (*Fig. 2.7*). Modification of proteins by incorporating such unnatural ferrocenyl amino acids helps the study of protein structure, activity and interaction with other biomolecules [38].

The ferrocenyl compounds are known to hold good potential as anticancer agents. This can be exemplified by the results obtained by the group of Gérard Jaouen, with the development of ferrocifens (i.e. ferrocene-modified tamoxifens), which exhibit strong antiproliferative effects not only in hormone dependent but also in hormone-independent breast cancer cells [39-48]. A recent review by Ca´tia Ornelas throws light on the various applications of ferrocene and its derivatives in cancer research [49].

Here we have synthesized a series of amino acid conjugated ferrocene mannich bases. These ferrocenyl amino acids have been targeted as it has been shown that tethering biologically active groups to the ferrocenyl unit increases their potency, possibly due to the combined action of the organic molecule with Fenton chemistry of the Fe-centre [50,51].

2.3.2 Materials and instrumentation:

All the chemicals and solvents used for synthesis and characterization of ligands are of analytical grade and were used as purchased. Ferrocene carboxaldehyde was purchased from Sigma Aldrich and amino acids were purchased from SRL (Sisco research laboratory, Mumbai, India.). All the solvents used in the present studies were purchased from Merck and are of analytical grade.

^{1}H NMR spectra, infrared spectra and UV spectra were recorded on the same instrument models as mentioned previously (*sec. 2.2.2*). ESI Mass spectra were recorded on Applied Biosystem API 2000 Mass spectrometer.

2.3.3 Synthesis and characterization:

The ferrocenyl amino acids **FcA 1-4** were synthesized according to a procedure reported by Chakravarty *et al* [52]. Amino acid (2.76 mmol) and NaOH (2.76 mmol) in dry methanol (5 ml) were stirred for 30 min to get a homogeneous solution. A methanolic solution (5 ml) of ferrocene carboxaldehyde (2.76 mmol) was added dropwise to the above solution, which was refluxed for 90 min, cooled, and treated with sodium borohydride (5.2 mmol) with constant stirring. The solvent was evaporated, the resulting mass was dissolved in water and acidified with dilute HCl, and the solution pH was maintained within 5-6. The ligand that precipitated as a yellow solid was filtered, thoroughly washed with water and cold methanol, and finally dried in vacuum. Yields of all the four ligands were in the range of 80-90%.

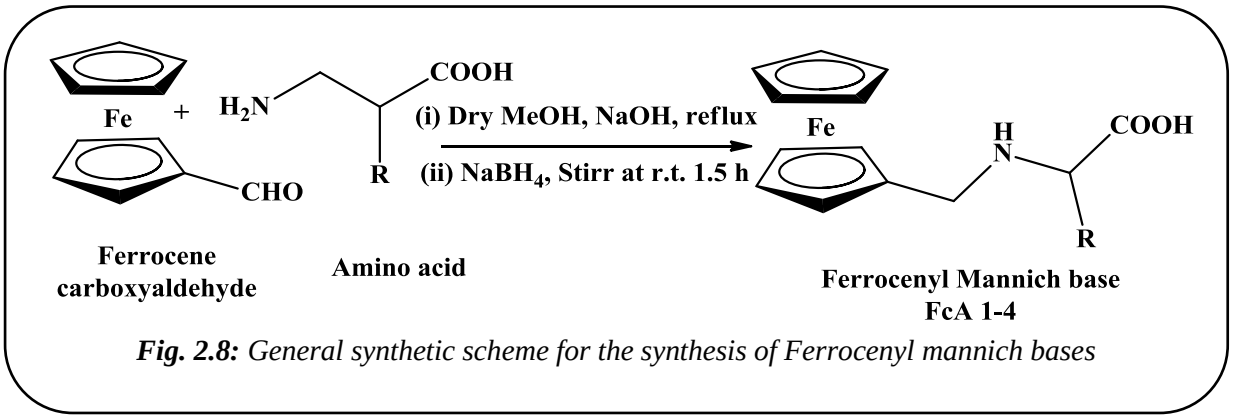

Fig. 2.8: *General synthetic scheme for the synthesis of Ferrocenyl mannich bases*

N-ferrocenyl-Tyrosine (**FcA-1**)

FcA-1 was prepared by condensation of Ferrocene carboxaldehyde (2.76 mmol, 590 mg) and tyrosine (2.76 mmol, 500 mg) followed by $NaBH_4$ reduction. Pale yellow powder was obtained. Solubility: DMSO, DMF; Yield 86.12 %; Molecular Weight 379.23 g/mol; Molecular Formula $C_{20}H_{21}FeNO_3$; MS *m/z*: 378.4 (M^+-1); FTIR (KBr)/cm^{-1} ν_{O-H} 3420(b), ν_{N-H} 3095(m), $\nu_{C=O}$ 1580(s).

N-ferrocenyl-Phenyl alanine (**FcA-2**)

FcA-2 was prepared by condensation of Ferrocene carboxaldehyde (2.76 mmol, 590 mg) and phenyl alanine (2.76 mmol, 455 mg) followed by $NaBH_4$ reduction. Pale yellow powder was obtained. Solubility: DMSO, DMF; Yield 79.62 %; Molecular Weight

363.23 g/mol; Molecular Formula $C_{20}H_{21}FeNO_2$; MS *m/z*: 362.1 (M^+-1); FTIR (KBr)/cm^{-1} ν_{O-H} 3422(b), ν_{N-H} 3028(m), $\nu_{C=O}$ 1612(s).

N-ferrocenyl-Leucine (**FcA-3**)

FcA-3 was prepared by condensation of Ferrocene carboxaldehyde (2.76 mmol, 590 mg) and leucine (2.76 mmol, 362 mg) followed by $NaBH_4$ reduction. Pale yellow powder was obtained. Solubility: DMSO, DMF; Yield 81.79 %; Molecular Weight 329.22 g/mol; Molecular Formula $C_{17}H_{23}FeNO_2$; MS *m/z*: 328.4 (M^+-1); FTIR (KBr)/cm^{-1} ν_{O-H} 3462(b), ν_{N-H} 2956(m), $\nu_{C=O}$ 1603(s).

N-ferrocenyl-Tryptophan (**FcA-4**)

FcA-4 was prepared by condensation of Ferrocene carboxaldehyde (2.76 mmol, 590 mg) and tryptophan (2.76 mmol, 563 mg) followed by $NaBH_4$ reduction. Pale yellow powder was obtained. Solubility: DMSO, DMF; Yield 89.12 %; Molecular Weight 402.27 g/mol; Molecular Formula $C_{22}H_{22}FeN_2O_2$; MS *m/z*: 401.3 (M^+-1); FTIR (KBr)/cm^{-1} ν_{O-H} 3444(b), ν_{N-H} 2925(m), $\nu_{C=O}$ 1597(s).

2.3.4 Results and discussion:

The four ferrocenyl mannich bases have been synthesized according to the general synthetic route given in *Fig. 2.8* in good yields.

The composition and structures of all the four hydrazones have been confirmed by ^1H NMR, Mass spectrometry, infrared spectroscopy and UV-Vis spectroscopy. The analytical data are consistent with the proposed structures and their empirical formulas.

The IR spectra of the ligands **FcA 1-4** displayed characteristic strong stretching bands at 1580-1610 cm^{-1} due to C=O of the carboxylic acid group. A distinct broad band at ~3450 cm^{-1} owing to the O-H stretching of free carboxylic acid group is found. The medium secondary amine N-H stretching bands are also found in the region of 2900-3000 cm^{-1}.

The UV spectra of the ligands **FcA 1-4** in DMSO (*Fig. 2.9*) was carried out in the region 200-400 nm. All the ligands show peaks ascribed to $\pi \rightarrow \pi^*$ intra ligand transition of the cyclopentadienyl rings of ferrocene at around 207-209 nm. Very low intensity $n \rightarrow \pi^*$ bands are obtained in the region 265-295 nm which has been shown as an expansion in the inset of *Fig. 2.9*. The peak values have been tabulated in *Table 2.2*.

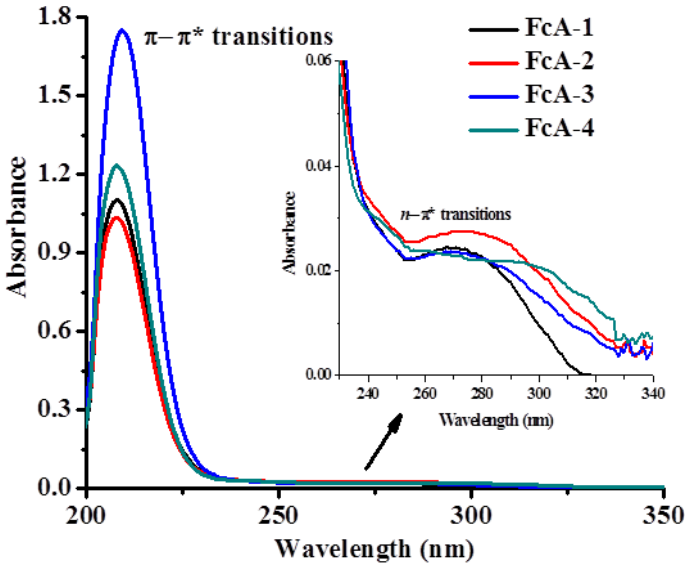

Fig. 2.9: *UV spectra of ligands* ***FcA 1-4*** *recorded in DMSO with path length 1 cm. (Inset: Expanded spectra showing the low intensity bands corresponding to n→π*)*

Table 2.2: *UV peak assignments of* ***FcA 1-4***

Compound	***Intra-ligand Transitions (nm)***	
	π-π*	***n-π****
FcA-1	207	271
FcA-2	208	273
FcA-3	209	268
FcA-4	208	294

The ^{1}H NMR spectra of ligands **FcA-3** and **FcA-4** show 9 proton multiplet in the δ range of 4-5 ppm that can be ascribed to the ferrocenyl ring protons. The singlet signals at δ= 11-12 ppm pertains to the N-H and COO-H proton of the amino acid. The spectrum of **FcA-3** (*Fig. 2.10, A*), apart from the above mentioned signals, also shows a 6 proton singlet at δ = 1.2 ppm owing to two methyl groups –CH(CH_3)$_2$ of leucine. Whereas the spectrum of **FcA-4** (*Fig. 2.10, B*) shows a 5 proton multiplet in the δ range of 7-8 ppm ascribable to the aromatic protons of the tryptophan and a one proton singlet at δ = 11 ppm attributed to the indoyl N-H. Due to poor solubility of the ligands, good resolved NMR spectra could not be achieved and those of **FcA-1** and **FcA-2** are not clear at all hence are not discussed here.

The ESI-MS spectra of the ligands **FcA 1-4** (*Fig. 2.11*) showed molecular ion peaks at *m/z* values equal to (M^{+}-1) which is in well agreement with the proposed composition.

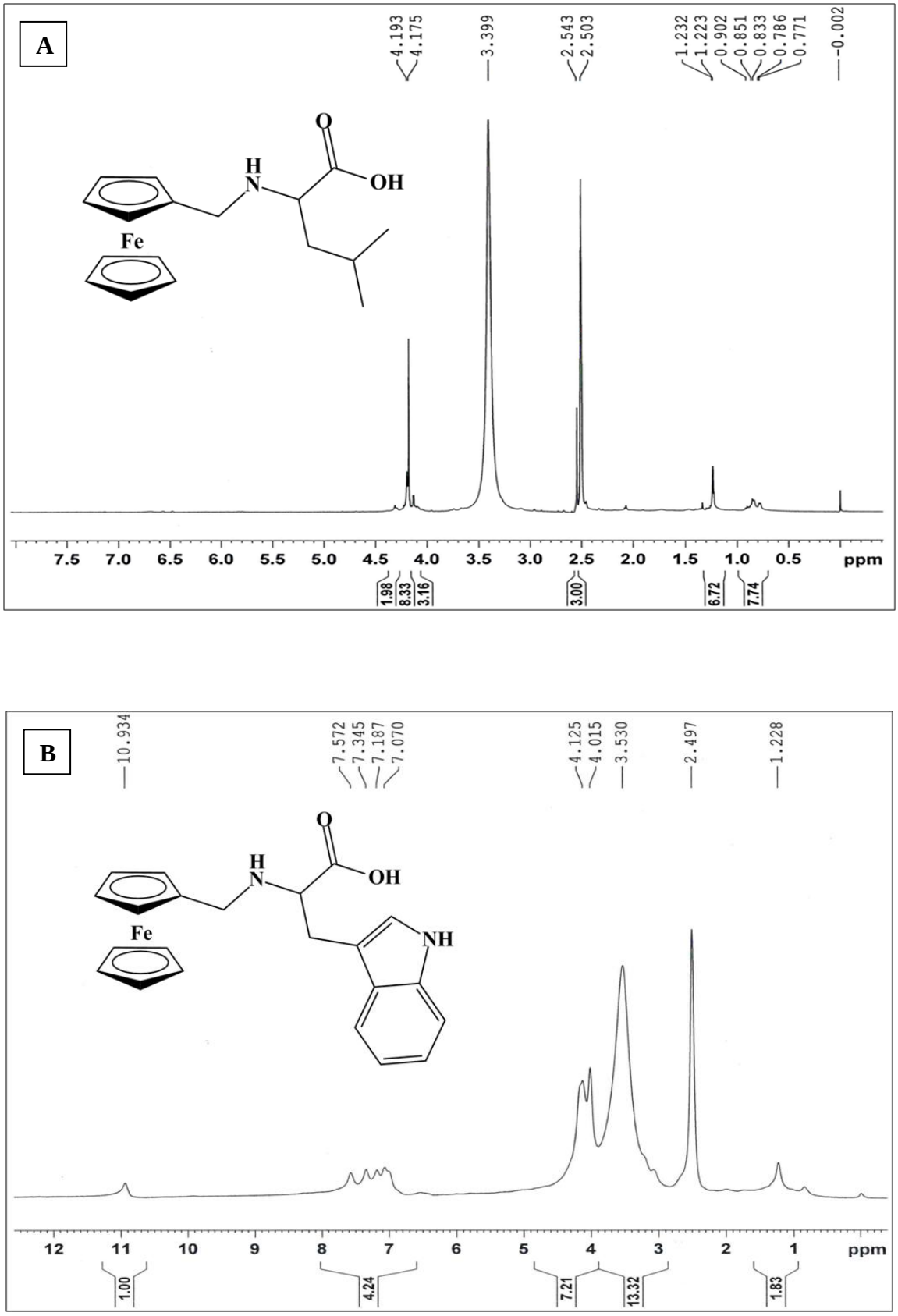

Fig. 2.10: *^{1}H NMR spectra of ligands (A)* ***FcA-3*** *(B)* ***FcA-4***

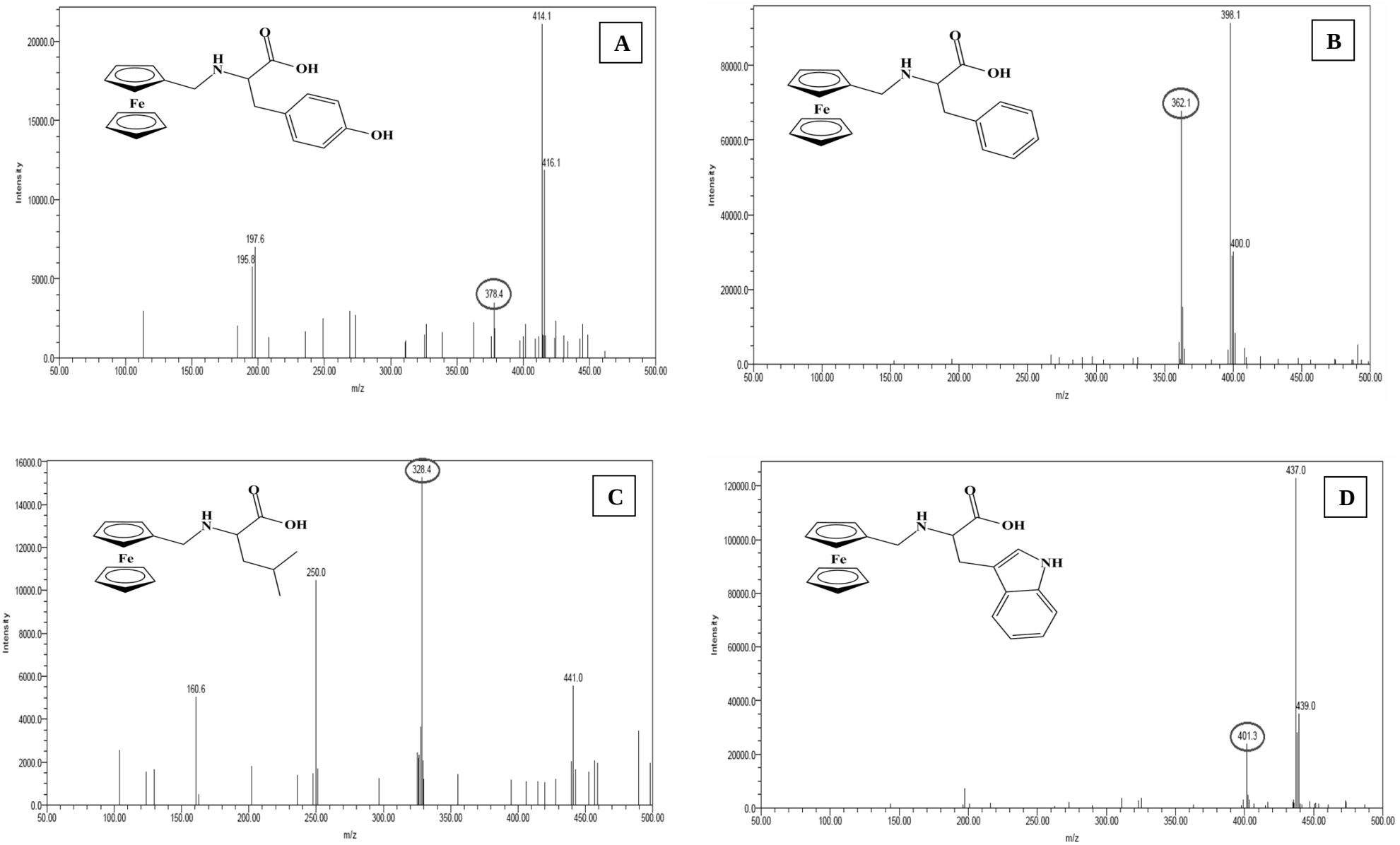

Fig. 2.11: *ESI Mass spectra of ligands (A)* ***FcA-1*** *(B)* ***FcA-2*** *(C)* ***FcA-3*** *(D)* ***FcA-4*** *indicating the molecular ion peak.*

2.4 Stilbene derivatives

2.4.1 Introduction:

Stilbenoids are a class of natural compounds, formed by a particular branch of the flavonoid biosynthetic pathway. Being first isolated from plants in 1899, they attracted the scientific community attention due to their chemical diversity and wide range of biological effects [53]. Nowadays it is widely accepted, that stilbenoids play an important role as phytoalexins in plant resistance to fungal pathogens [54]. Recently, natural hydroxy stilbenes (a particular group of stilbenoids) such as resveratrol and combretastatin, as well as their synthetic analogues, become of a great interest to the medicinal chemists. These compounds have been proved to be antioxidant reagents, that inhibit cell apoptosis, suppress growing cancer cells, influence the activity of specific enzymes, affect the animal ageing and metabolisms of estrogens [55-58] etc. Resveratrol (3,4,5-trihydroxystilbene) is a polyphenolic natural product. It harbors a stilbene structure and belongs to the group of phytoalexins that become activated under stress conditions of plants. These compounds exist in foods and beverages (e.g. in grapes and red wine) and are widely consumed. Resveratrol is also classified as a phytoestrogen because of its ability to interact with estrogen receptors. In addition, it is related to the synthetic estrogen diethylstilbestrol. Resveratrol exerts various biological activities that are beneficial to human health, including chemopreventive, anti-inflammatory, antioxidant, antiproliferative, proapoptotic, cardioprotective and anticancer properties [59]. Although the hydroxy stilbenoids possess remarkable medical benefits, it is noteworthy that their bioavailability is very narrow. In fact they are only produced in nanogram scale in plants, in response to stress situations such as fungal infection or injury, and thus, it is hardly to be obtained in large quantities from their natural sources. To overcome this, various synthetic approaches for the synthesis of stilbenes have been developed.

In the current study we have synthesized a series of stilbene derivatives containing pyridyl ring as one of the aromatic rings using Wittig-Heck reaction.

2.4.2 Materials and instrumentation:

All the chemicals and solvents used for synthesis and characterization of ligands are of analytical grade and were used as purchased. Vinyl pyridine, aryl halides and palladium catalyst were purchased from Sigma Aldrich. All the solvents used in the present studies were purchased from Merck and are of analytical grade.

^{1}H NMR spectra, mass spectra, infrared spectra and UV spectra were recorded on the same instrument models as mentioned previously (*sec. 2.2.2*).

2.4.3 Synthesis and characterization:

All four stilbene derivatives **Stb 1-4** were synthesized according to a procedure reported by Krupa *et al* [60]. Aryl halide, vinyl pyridine and K_2CO_3 were taken in the mole ratio of 1:1.05:2 respectively along with $Pd(OAc)_2$ (0.5%), dppp (1%) and TBAB (10%) in 5-6 ml DMA in a single pot. The reaction mixture was refluxed for 40 h. On completion of reaction, the reaction mixture was dumped in water followed by product extraction in methylene dichloride. The crude product so obtained was purified using column chromatography.

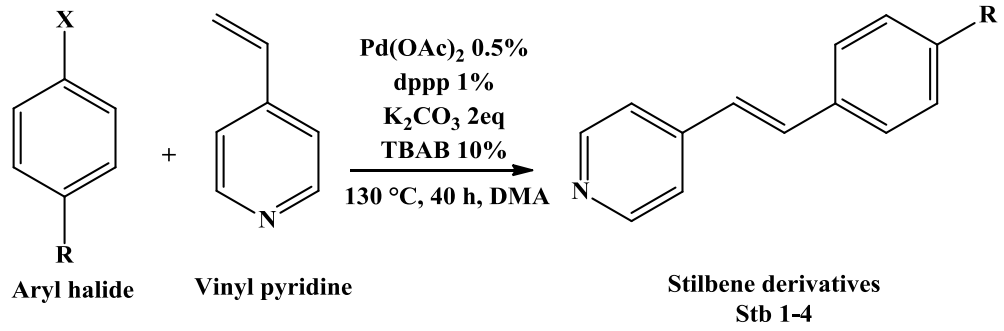

***Fig. 2.12**: General synthetic scheme for the synthesis of stilbene derivatives.*

((E)-4-styrylpyridine) (**Stb-1**)

Stb-1 was prepared by condensation of iodobenzene (0.98 mmol, 200 mg) and vinyl pyridine (1.03 mmol, 108 mg) in presence of Pd catalyst and other reagents. Pale yellow crystals were obtained. Solubility: MeOH, DMSO, DMF; Yield 68.70 %, mp 134°C; Molecular Weight 181.23 g/mol; Molecular Formula $C_{13}H_{11}N$; MS *m/z*: 180.26 (M^+-1); δ_H (400 MHz, $CDCl_3$) 8.60 (d, *J* 6.3, 2H, pyridyl α-H), 7.57-7.55 (dd, J_1 1.6, J_2 7.8, 2H, pyridyl β -H), 7.41-7.36 (m, 5H, Ar-H), 7.34 (d, J_{trans} 16.4, 1H, HC=CH), 7.06 (d, J_{trans} 16.4, 1H, HC=CH); δ_C (400 MHz, $CDCl_3$) 150.2, 144.6, 136.1, 133.2, 128.8, 128.7, 127.0, 125.9, 120.8; FTIR (KBr)/cm^{-1} ν_{ArC-H} 3025(w), $\nu_{C=N(py)}$ 1500, $\nu_{ArC=C}$ 1588(s), 1549(sh), 1493(m), 1453(m).

((E)-4-(4-methoxystyryl)pyridine) (**Stb-2)**

Stb-2 was prepared by condensation of 4-iodoanisole (0.85 mmol, 200 mg) and vinyl pyridine (0.89 mmol, 94 mg) in presence of Pd catalyst and other reagents. Pale yellow crystals were obtained. Solubility: MeOH, DMSO, DMF; Yield 73.21 %, mp 138°C; Molecular Weight 211.26 g/mol; Molecular Formula $C_{14}H_{13}NO$; MS *m/z*: 211.07 (M^+); δ_H (400 MHz, $CDCl_3$) 8.57 (d, *J* 6, 2H, pyridyl α-H), 7.51-7.49 (dd, J_1 1.6, J_2 6.8, 2H,

pyridyl β -H), 7.36-7.34 (dd, J_1 1.2, J_2 4.4, 2H, Ar-H), 7.29 (d, J_{trans} 16.4, 1H, HC=CH), 6.95-6.93 (dd, J_1 2, J_2 6.8, 2H, Ar-H), 6.92 (d, J_{trans} 16.4, 1H, HC=CH), 3.86 (s, 3H, -OCH_3); δ_C (400 MHz, $CDCl_3$) 160.1, 150.1, 144.9, 132.7, 128.8, 128.4, 123.7, 120.6, 114.2, 55.3; FTIR (KBr)/cm^{-1} ν_{ArC-H} 3020(w), $\nu_{C=N(py)}$ 1508(s), $\nu_{ArC=C}$ 1585(s), 1456(m), 1411(m), ν_{C-O} 1172(s).

((E)-4-(4-nitrostyryl)pyridine) (**Stb-3**)

Stb-3 was prepared by condensation of 4-iodonitrobenzene (0.91 mmol, 200 mg) and vinyl pyridine (0.96 mmol, 101 mg) in presence of Pd catalyst and other reagents. Pale yellow crystals were obtained. Solubility: MeOH, DMSO, DMF; Yield 77.53 %, mp 154°C; Molecular Weight 226.23 g/mol; Molecular Formula $C_{13}H_{10}N_2O_2$; MS *m/z*: 225.73 (M^+); δ_H (400 MHz, $CDCl_3$) 8.66 (d, *J* 4.8, 2H, pyridyl α-H), 8.28-8.26 (dd, J_1 1.6, J_2 6.8, 2H, pyridyl β -H), 7.71-7.69 (dd, J_1 1.6, J_2 6.8, 2H, Ar-H), 7.47 (d, *J* 6, 2H, Ar-H), 7.39 (d, J_{trans} 16.4, 1H, HC=CH), 7.22 (d, J_{trans} 16.4, 1H, HC=CH); δ_C (400 MHz, $CDCl_3$) 149.6, 147.5, 144.1, 142.3, 131.1, 130.2, 127.5, 124.2, 121.3; FTIR (KBr)/cm^{-1} ν_{ArC-H} 3053(w), $\nu_{C=N(py)}$ 1507(s), $\nu_{ArC=C}$ 1597(s), 1561(sh), 1415(m), ν_{N-O} 1340(s).

((E)-4-(4-fluorostyryl)pyridine) (**Stb-4**)

Stb-4 was prepared by condensation of 4-bromofluorobenzene (2.85 mmol, 500 mg) and vinyl pyridine (2.99 mmol, 314 mg) in presence of Pd catalyst and other reagents. Pale yellow crystals were obtained. Solubility: MeOH, DMSO, DMF; Yield 81.91 %, mp 118°C; Molecular Weight 199.22 g/mol; Molecular Formula $C_{13}H_{10}FN$; MS *m/z*: 199.16 (M^+); δ_H (400 MHz, $CDCl_3$) 8.59 (d, 2H, pyridyl α-H), 7.54-7.51 (dd, 2H, pyridyl β -H), 7.37 (d, 2H, Ar-H), 7.29 (d, J_{trans} 16.4, 1H, HC=CH), 7.12-7.08 (dd, 2H, Ar-H), 6.96 (d, J_{trans} 16.4, 1H, HC=CH); δ_C (400 MHz, $CDCl_3$) 164.1, 150.2, 144.4, 132.3, 131.9, 128.7, 128.6, 125.7, 115.7; FTIR (KBr)/cm^{-1} ν_{ArC-H} 3054(w), $\nu_{C=N(py)}$ 1507(s), $\nu_{ArC=C}$ 1586(s), 1548(sh), 1408(s), ν_{C-F} 1157(s).

2.4.4 Results and discussion:

Lot of synthetic approaches for the synthesis of stilbene analogues have been developed including Colvin rearrangement to an alkyne, followed by selective semi-reduction [61], Suzuki cross-coupling [62,63], Heck [64], Wittig [65,66] and Perkin reactions [67,68], to name just a few. It is however rather important to be mentioned, that the formation of the carbon- carbon double bond between the two aromatic rings is the key step in all the synthetic approaches developed, but in most of the cases a mixture of cis- and trans- isomers is produced. Thus, additional work is required in order these

isomeric mixtures to be separated, which lowers the products' yields and limits the benefits of these approaches from an applied standpoint. Here the approach used for the synthesis of pyridyl stilbene derivatives is in situ one pot reaction with appropriate aryl halide and one carbon Wittig salt and then subjected to the palladium catalyzed Mizoroki–Heck reaction (*Fig. 2.12*). In this protocol the Mizoroki–Heck step determines the stereochemistry of alkene and as expected the product was predominantly formed as E isomer [60].

The composition and structures of all the four stilbene derivatives have been confirmed by ^{1}H and ^{13}C NMR, Mass spectrometry, infrared spectroscopy and UV-Vis spectroscopy. The analytical data are consistent with the proposed structures and their empirical formulas.

The IR spectra of **Stb 1-4** typically show aromatic C-H stretching near 3000 cm^{-1} and aromatic ring C=C in plane vibrations in the region 1660-1430 cm^{-1}. Strong band at around 1500-1508 cm^{-1} is found owing to the C=N stretching of the pyridine ring. Further the bands in the region 830-850 cm^{-1} are indicative of *p*-disubstituted aromatic rings.

The UV spectra of all the four ligands show absorption bands in the wavelength range 200-350 nm (*Fig. 2.13*). The peaks around 220-225 nm are due to the intra-ligand aromatic ring centered $\pi \rightarrow \pi^*$ and those observed around 300-340 nm are owing to the $n \rightarrow \pi^*$ transitions. The λ_{max} of the ligands varies depending on the ring substitution. The peak values have been tabulated in *Table 2.3*.

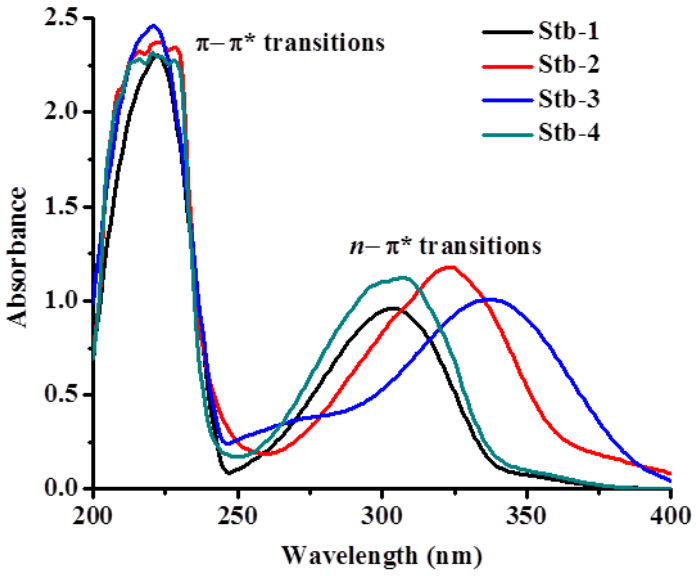

Fig. 2.13: *UV spectra of ligands* ***Stb 1-4*** *recorded in DMSO with path length 1 cm.*

Table 2.3: *UV peak assignments of* ***Stb 1-4***

Compound	***Intra-ligand Transitions (nm)***	
	π-π*	***n-π****
Stb-1	224	303
Stb-2	221	323
Stb-3	222	337
Stb-4	221	305

The mass spectra of ligands **Stb 1-4** show good intensity peaks corresponding to the molecular ions M^+ at *m/z* = 180.26, 211.07, 225.73 and 199.16 respectively (*Fig. 2.14*).

The ^{1}H NMR spectra of all the four stilbene derivatives (*Fig. 2.15*) show pyridyl peaks for α and β protons at δ ~ 8.6 ppm and ~ 7.5 ppm respectively. The two, single proton, doublets in the region 6.9-7.35 ppm with coupling constant *J* = 16.4 confirms the formation of *trans* alkene (HC=CH) via wittig-heck condensation between vinyl pyridine and substituted aryl halide. Additionally a 3 proton singlet at δ = 3.86 ppm in case of **Stb-2** corresponds to the methoxy group on the phenyl ring whereas the nitro and fluoro substituents in case of **Stb-3** and **4** respectively led to different splitting in the aryl proton signals.

^{13}C NMR spectra of **Stb 1-4** given in *Fig. 2.16* is in accordance with the proton NMR. The peaks at δ ~ 150, 126 and 134 ppm refer to α, β and γ carbons on the pyridyl ring. Peaks at 133 and 128 ppm correspond to HC=CH carbons. Rest of the peaks can be attributed to the phenyl ring carbons which vary with substituents. **Stb-2** containing a methoxy group shows a shift in its aryl peaks with C1 and C2 obtained at δ = 160.1 and 114.2 ppm respectively with respect to the methoxy substituent. Moreover a peak at 55.3 ppm ascribable to methoxy carbon confirms the presence of -OMe on the phenyl ring. In case of **Stb-3** the C1 carbon gives rise to peak at δ = 147.5 ppm and C2 at 124.2 ppm owing to a nitro substitution. Similarly in case of **Stb-4** with fluoro substitution the peaks for C1 and C2 with respect to fluoro group are obtained at 164 and 115.7 ppm respectively.

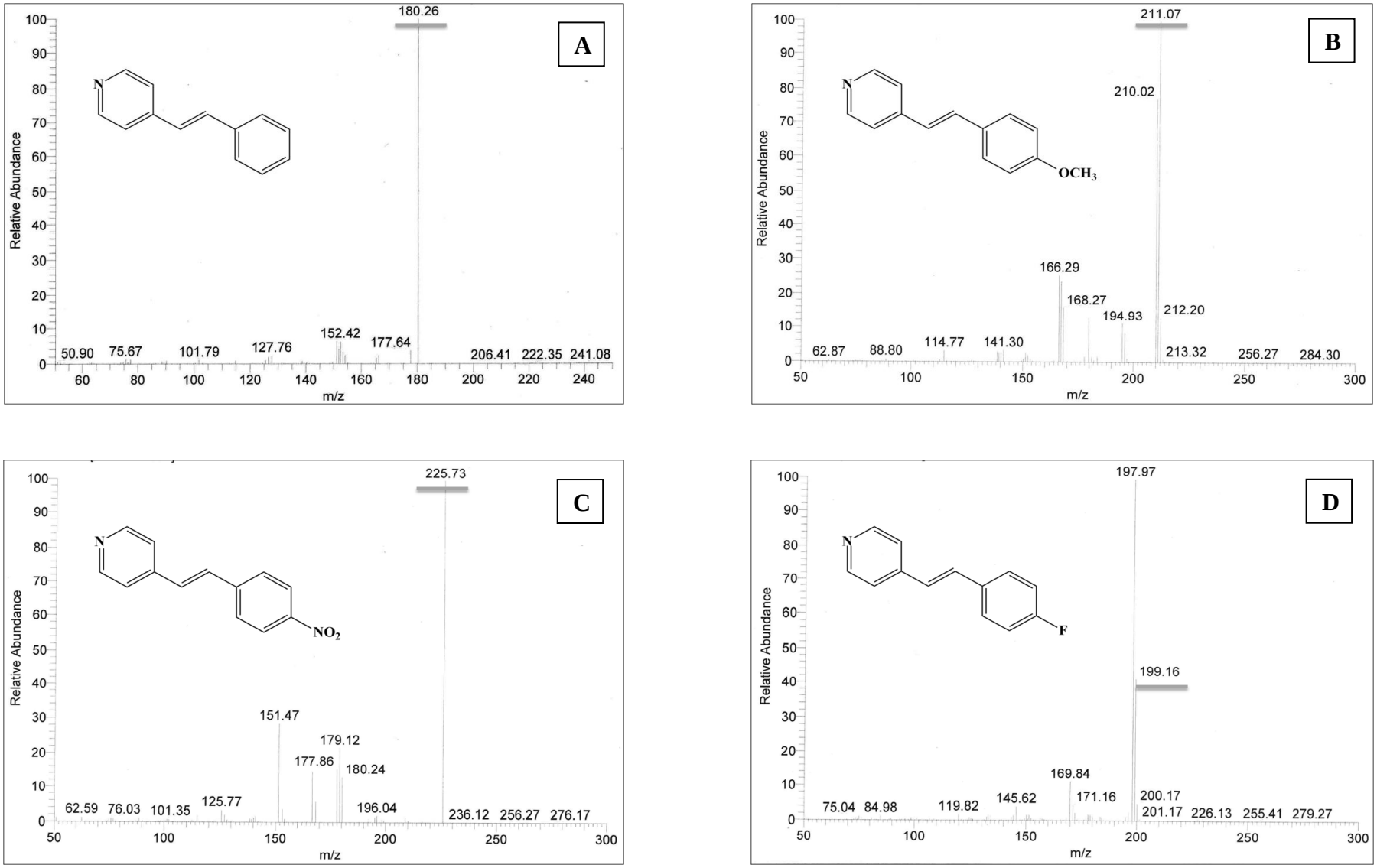

Fig. 2.14: *Mass spectra of ligands (A)* ***Stb-1*** *(B)* ***Stb-2*** *(C)* ***Stb-3*** *(D)* ***Stb-4*** *indicating the molecular ion peak.*

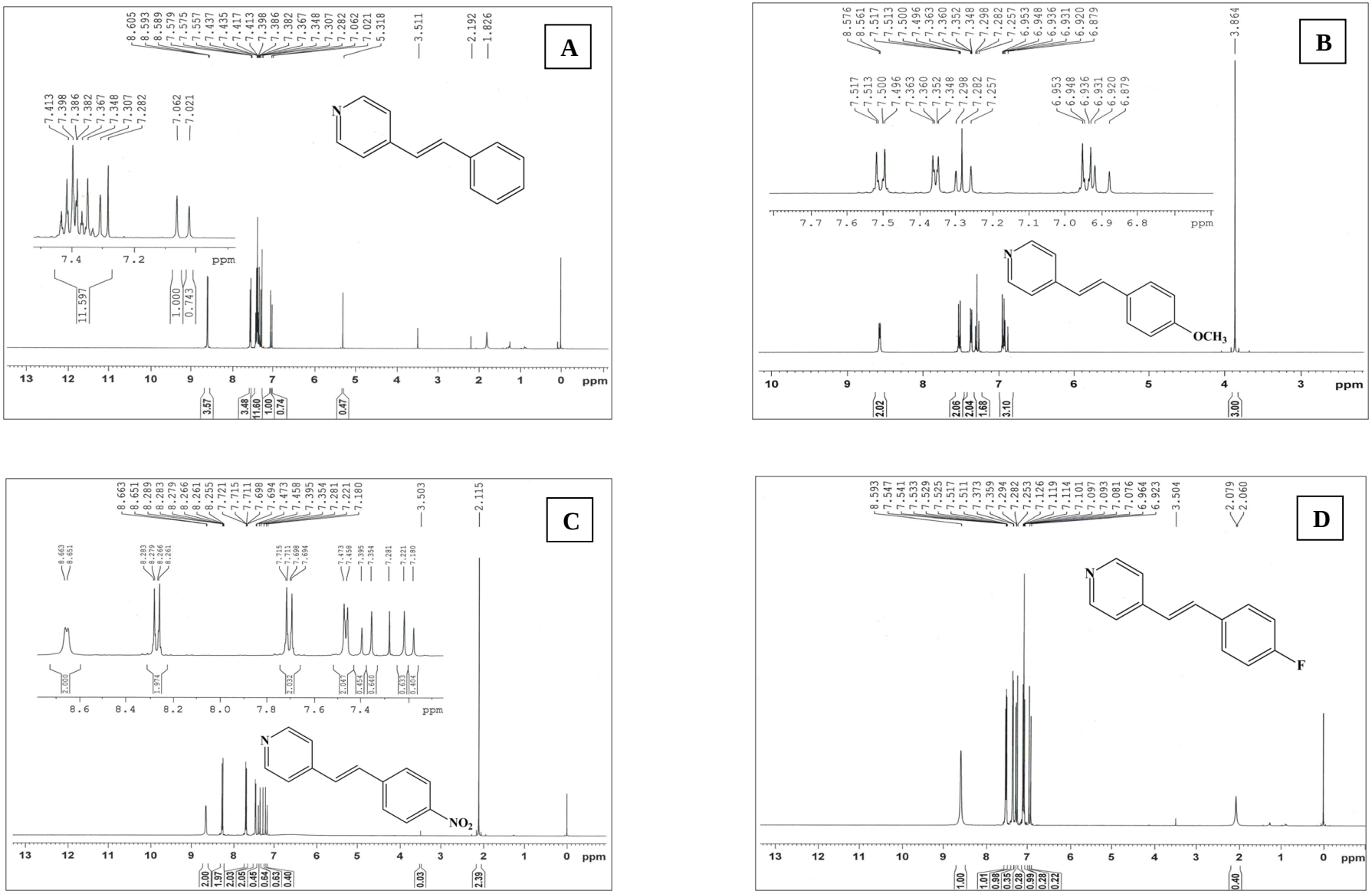

Fig. 2.15: *^{1}H NMR spectra of ligands (A)* ***Stb-1*** *(B)* ***Stb-2*** *(C)* ***Stb-3*** *(D)* ***Stb-4***

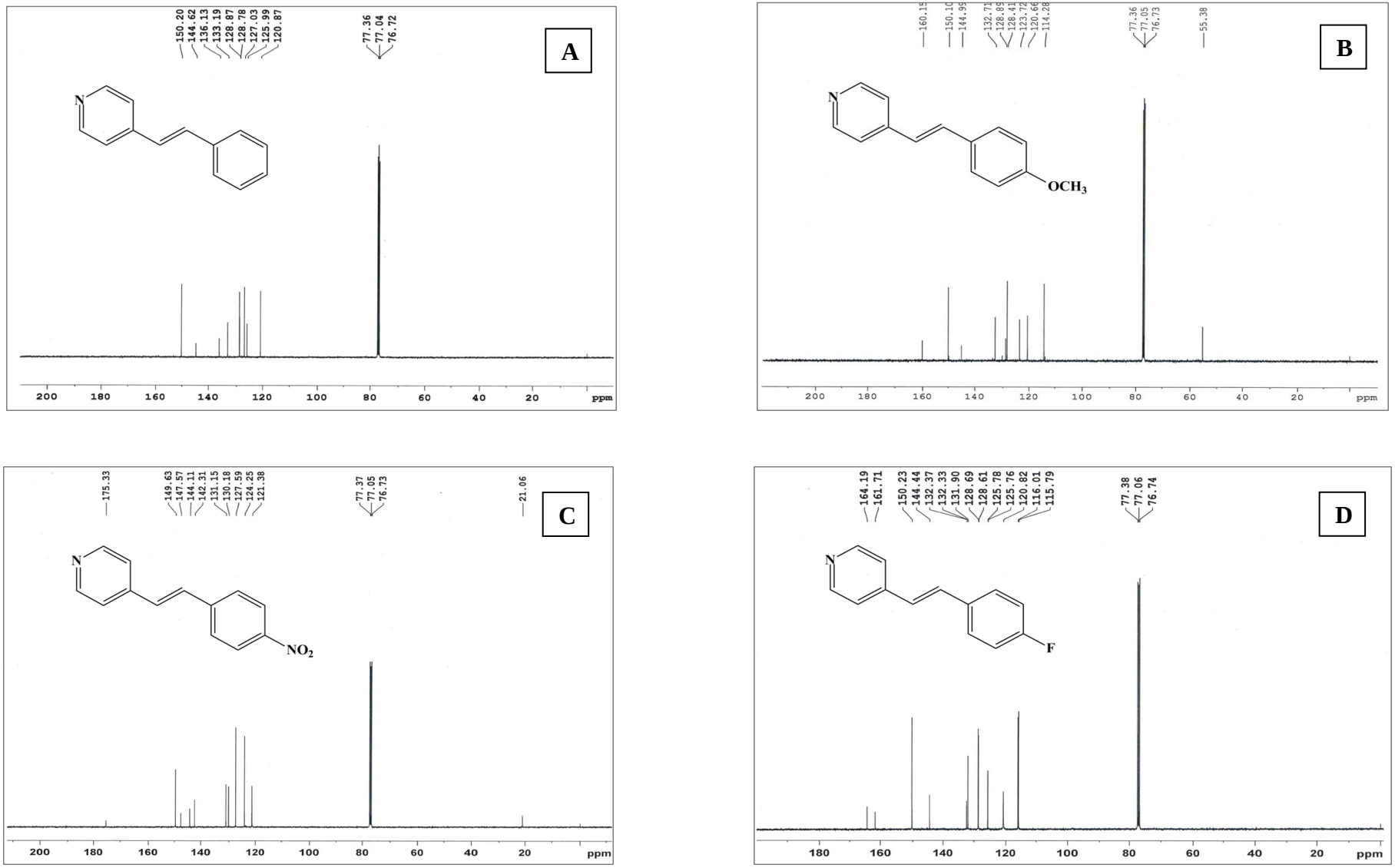

Fig. 2.16: *^{13}C NMR spectra of ligands (A)* ***Stb-1*** *(B)* ***Stb-2*** *(C)* ***Stb-3*** *(D)* ***Stb-4***

2.5 Isatin Schiff bases

2.5.1 Introduction:

Isatin (2,3-dioxindoles) is a natural product found in a number of plants and has been found as a metabolic derivative of adrenaline in humans. Substituted isatins are also found naturally in plants. Isatin and its derivatives are widely used as starting materials for the synthesis of a broad range of heterocyclic compounds and as substrates for drug synthesis. The importance of the indole nucleus is well established in the field of pharmaceutical chemistry, in plants and animal biochemistry. Isatin and its various derivatives are known to possess a wide range of pharmacological and biological properties [69]. Recently these heterocycles have been shown to demonstrate antiprotozoal, antibacterial, antifungal, antiviral, anti-HIV, anticonvulsant, antitumoral, anti-inflammatory, and antihelminthic activities; influence neurodegenerative diseases; participate in metabolism; acetylcholinesterase inhibitors; and stimulate the growth of plants. Drugs containing the isatin skeleton are used to treat diseases such as epilepsy, tuberculosis, and bulimia. Therefore the need to create novel isatin derivatives for emerging drug targets is an active area of medicinal chemistry [70]. Many Isatin derivatives, such as isatin hydrazones, isatin mannich bases, isatin based spiroazetidinones and 3-(methylene)indolin-2-ones, have also been reported to possess neuro-protection activity [71]. Within the context of enzyme inhibitors, isatins have seen recent applications in the inhibition of cysteine and serine proteases. Isatin-3-isonicotinylhydrazone was screened against *Mycobacterium tuberculosis* and was found to be more sensitive than isoniazid and isatin drugs. The minimum inhibitory concentration (MIC) results of this compound proved its higher potency and may be recognized as a suitable antitubercular agent [72].

Isatin-3-thiosemicarbazone, isatin-3 isonicotinylhydrazone and their derivatives revealed significant growth inhibitory activity against the tested *Mycobacterium tuberculosis* MTB H37Rv strains. Moreover, isatin-3-isonicotinylhydrazone was evaluated *in vitro* as an antimicrobial agent against representative strains of gram-positive bacteria as well as good CT-DNA intercalator. Also 1-methylisatin 3-thiosemicarbazone (methisazone) is clinically used as an antiviral agent [72]. The vast medicinal activity of the isatin hydrazones prompted us to prepare a series of isatin Schiff bases with an aim to check their potency on cancer cell lines.

2.5.2 Materials and instrumentation:

All the chemicals and solvents used for synthesis and characterization of ligands are of analytical grade and were used as purchased. Isatin was purchased from Acros organics whereas the hydrazines were purchased from SRL (Sisco research laboratory, Mumbai, India.). All the solvents used in the present studies were purchased from Merck and are of analytical grade.

^{1}H NMR spectra, mass spectra, infrared spectra and UV spectra were recorded on the same instrument models as mentioned previously (*sec. 2.2.2*).

2.5.3 Synthesis and characterization:

All four isatin Schiff bases **Isa 1-4** were synthesized according to a reported procedure [70]. Isatin and the respective hydrazide were taken in the mole ratio of 1:1 in 20 ml absolute ethanol, few drops of glacial acetic acid were added as catalyst and refluxed for 4 h. On cooling the solid crystalline product was obtained which was filtered and recrystallized from absolute ethanol.

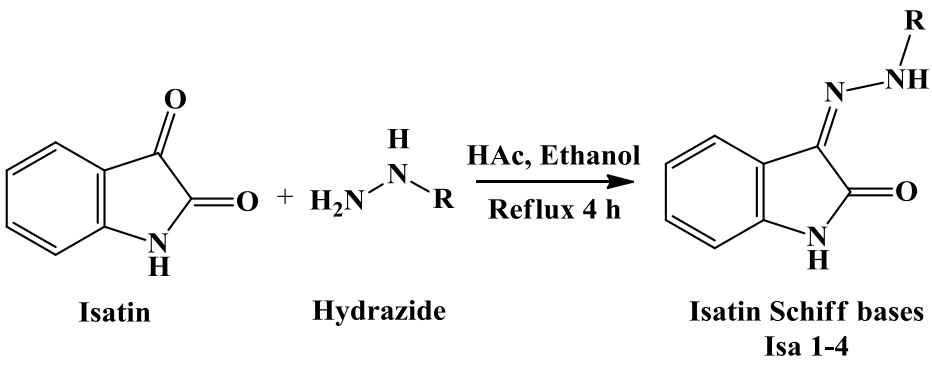

***Fig. 2.17**: General synthetic scheme for the synthesis of Isatin derivatives.*

(N'-(2-oxoindolin-3-ylidene)benzohydrazide) (**Isa-1**)

Isa-1 was prepared by condensation of isatin (6.8 mmol, 1000 mg) and benzoyl hydrazine (6.8 mmol, 925 mg) in presence of a few drops of glacial acetic acid. Pale yellow crystals were obtained. Solubility: DMSO, DMF; Yield 60.55%, mp 235°C; Molecular Weight 265.27 g/mol; Molecular Formula $C_{15}H_{11}N_3O_2$; MS *m/z*: 265.08 (M^+); δ_H (400 MHz, DMSO-d_6) 13.95 (s, 1H, N=NH), 11.39 (s, 1H, indolinic NH), 7.91-7.89 (dd, J_1 1.2, J_2 8.4, 1H, indolinic Ar-H), 7.69-7.60 (m, 5H, Ar-H), 7.42-7.38 (dt, J_1 1.2, J_2 7.6, 1H, indolinic Ar-H), 7.14-7.10 (t, *J* 7.6, 1H, indolinic Ar-H), 6.97-6.95 (d, *J 8* , 1H, indolinic Ar-H); FTIR (KBr)/cm^{-1} $\nu_{(amide)N-H}$ 3465(b), $\nu_{(indolinic)N-H}$ 3234(b), $\nu_{(indolinic)C=O}$ 1710(s), $\nu_{(amide)C=O}$ 1626(s), $\nu_{C=N}$ 1561(s)

(N'-(2-oxoindolin-3-ylidene)isonicotinohydrazide) **(Isa-2)**

Isa-2 was prepared by condensation of isatin (6.8 mmol, 1000 mg) and isoniazid (6.8 mmol, 933 mg) in presence of a few drops of glacial acetic acid. Yellow crystals were obtained. Solubility: DMSO, DMF; Yield 87.8%; mp 299°C; Molecular Weight 266.25 g/mol; Molecular Formula $C_{14}H_{10}N_4O_2$; MS *m/z*: 266.17 (M^+); δ_H (400 MHz, DMSO-d_6) 14.00 (s, 1H, N=NH), 11.44 (s, 1H, indolinic NH), 8.87-8.85 (d, *J* 5.6, 2H, pyridinyl α-H), 7.78-7.77 (dd, J_1 1.6, J_2 4.4, 2H, pyridinyl β-H), 7.61 (broad s, 1H, indolinic Ar-H), 7.42-7.39 (t, *J* 7.6, 1H, indolinic Ar-H), 7.13-7.09 (t, *J* 7.6, 1H, indolinic Ar-H), 6.96-6.95 (d, *J* 7.6, 1H, indolinic Ar-H); FTIR (KBr)/cm^{-1} $\nu_{(indolinic)N-H}$ 3231(s), $\nu_{(indolinic)C=O}$ 1721(s), $\nu_{(amide)C=O}$ 1672(s), $\nu_{C=N}$ 1599(m).

(2-(2-oxoindolin-3-ylidene)hydrazinecarboxamide) (**Isa-3**)

Isa-3 was prepared by condensation of isatin (6.8 mmol, 1000 mg) and semicarbazide (6.8 mmol, 758 mg) in presence of a few drops of glacial acetic acid. Yellowish brown crystals were obtained. Solubility: DMSO, DMF; Yield 79.06%; mp 243°C; Molecular Weight 204.19 g/mol; Molecular Formula $C_9H_8N_4O_2$; MS *m/z*: 204.18 (M^+); δ_H (400 MHz, DMSO-d_6) 12.46 (s, 1H, N=NH), 11.04 (s, 1H, indolinic NH), 9.05 (s, 2H, NH_2), 7.60-7.55 (dt, J_1 1.2, J_2 7.6, 1H, indolinic Ar-H), 7.50-7.48 (d, *J* 7.6,, 1H, indolinic Ar-H), 7.08-7.04 (t, *J* 7.6, 1H, indolinic Ar-H), 6.91–6.89 (d, *J* 8, 1H, indolinic Ar-H); FTIR (KBr)/cm^{-1} $\nu_{(amide)N-H}$ 3622(m), $\nu_{(indolinic)N-H}$ 3163(b), $\nu_{(indolinic)C=O}$ 1724(s), $\nu_{(amide)C=O}$ 1675(s), $\nu_{C=N}$ 1609(s).

(2-(2-oxoindolin-3-ylidene)hydrazinecarbothioamide) (**Isa-4**)

Isa-4 was prepared by condensation of isatin (6.8 mmol, 1000 mg) and thiosemicarbazide (6.8 mmol, 1500 mg) in presence of a few drops of glacial acetic acid. Pale yellow crystals were obtained. Solubility: DMSO, DMF; Yield 89.37%; mp 259°C; Molecular Weight 220.25 g/mol; Molecular Formula $C_9H_8N_4OS$; MS *m/z*: 219.96 (M^+). δ_H (400 MHz, DMSO-d_6) 12.46 (s, 1H, N=NH), 11.21 (s, 1H, indolinic NH), 9.05 (s, 2H, NH_2), 7.65-7.64 (d, *J* 7.2, 1H, indolinic Ar-H), 7.36-7.32 (dt, J_1 1.2, J_2 7.6, 1H, indolinic Ar-H), 7.10-7.06 (t, *J* 7.6, 1H, indolinic Ar-H), 6.93–6.91 (d, *J* 8, 1H, indolinic Ar-H); FTIR (KBr)/cm^{-1} $\nu_{(amide)N-H}$ 3456(s), $\nu_{(indolinic)N-H}$ 3169(s,b), $\nu_{(indolinic)C=O}$ 1746(s), $\nu_{C=S}$ 1203(s), $\nu_{C=N}$ 1571(s).

2.5.4 Results and discussion:

The four isatin Schiff bases have been synthesized according to the general synthetic route given in *Fig. 2.17* in good yields.

The composition and structures of all the four isatin derivatives have been confirmed by ^{1}H NMR, Mass spectrometry, infrared spectroscopy and UV-Vis spectroscopy. The analytical data are consistent with the proposed structures and their empirical formulas.

The IR spectra of the isatin ligands typically show strong secondary amide carbonyl absorption at 1620-1680 cm^{-1} while **Isa-4** shows a strong thiocarbonyl stretch at 1203 cm^{-1}. Also the absorption at 1700-1750 cm^{-1} is due to the indolinic C=O. The $\nu_{C=N}$ band is obtained as a strong peak at around 1550-1600 cm^{-1}. The N-H stretching bands found in the range of 3150-3250 cm^{-1} can be attributed to the indolinic N-H whereas the broad bands found in the range of 3550-3600 cm^{-1} are due to the free amide N-H stretch.

The UV spectra of **Isa 1-4** recorded in DMSO within 200-400 nm show three prominent bands. The first band appearing at ~ 220 nm is attributable to $\pi \rightarrow \pi^*$ transitions while the medium intensity second and third bands in the wavelength range 260-360 nm are owing to the $n \rightarrow \pi^*$ transitions (*Fig. 2.18*). The λ_{max} of the ligands varies depending on the ring substitution. The peak values have been tabulated in *Table 2.4*.

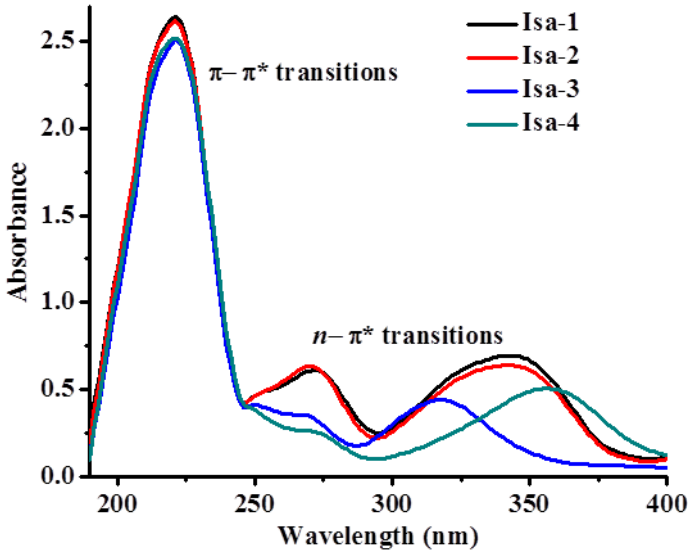

Fig. 2.18: *UV spectra of ligands* ***Isa 1-4*** *recorded in DMSO with path length 1 cm.*

Table 2.4: *UV peak assignments of* ***Isa 1-4***

Compound	***Intra-ligand Transitions (nm)***	
	π-π*	***n-π****
Isa-1	221	273, 344
Isa-2	221	271, 342
Isa-3	220	269, 317
Isa-4	220	272, 357

The mass spectra of the ligands (*Fig. 2.19*) show good intensities of their molecular ion peaks (M^+) at *m/z*: 265.08, 266.17, 204.18 and 219.96 respectively for **Isa 1-4**.

The ^1H NMR spectra of the ligands **Isa 1-4** (*Fig. 2.20*) are in well agreement with their proposed structures. The N-H proton of the diazenyl group (N=NH) shows a one proton singlet at a δ value of ~14-12.5ppm whereas the indolinic N-H shows a one proton singlet at a δ value of ~11.4-11.2 ppm confirming the condensation of isatin with hydrazides. Rest of the signals can be attributed to the aromatic protons of the indolinic ring and the substitution on the diazenyl group.

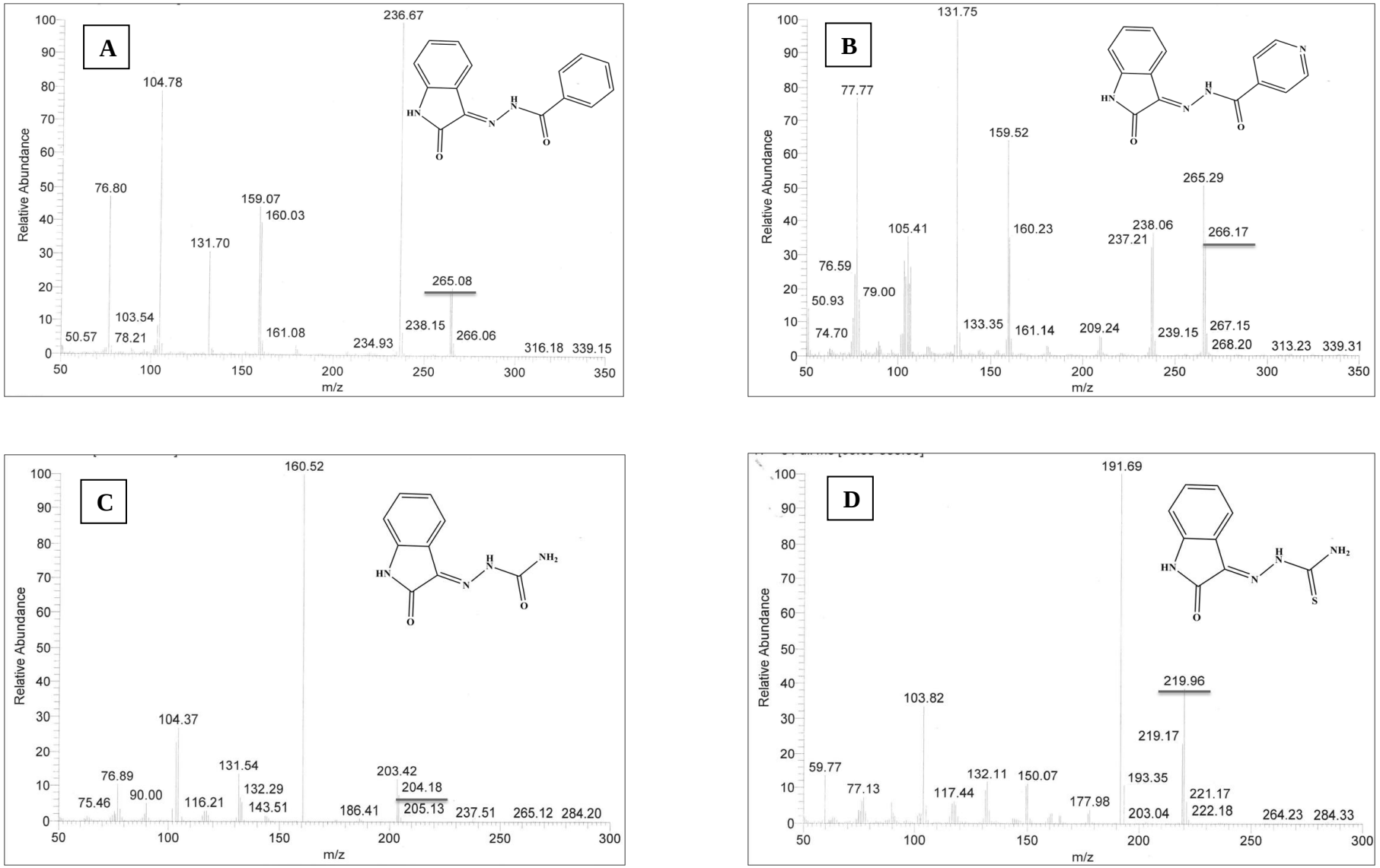

Fig. 2.19: *Mass spectra of ligands (A)* ***Isa-1*** *(B)* ***Isa-2*** *(C)* ***Isa-3*** *(D)* ***Isa-4*** *indicating the molecular ion peak.*

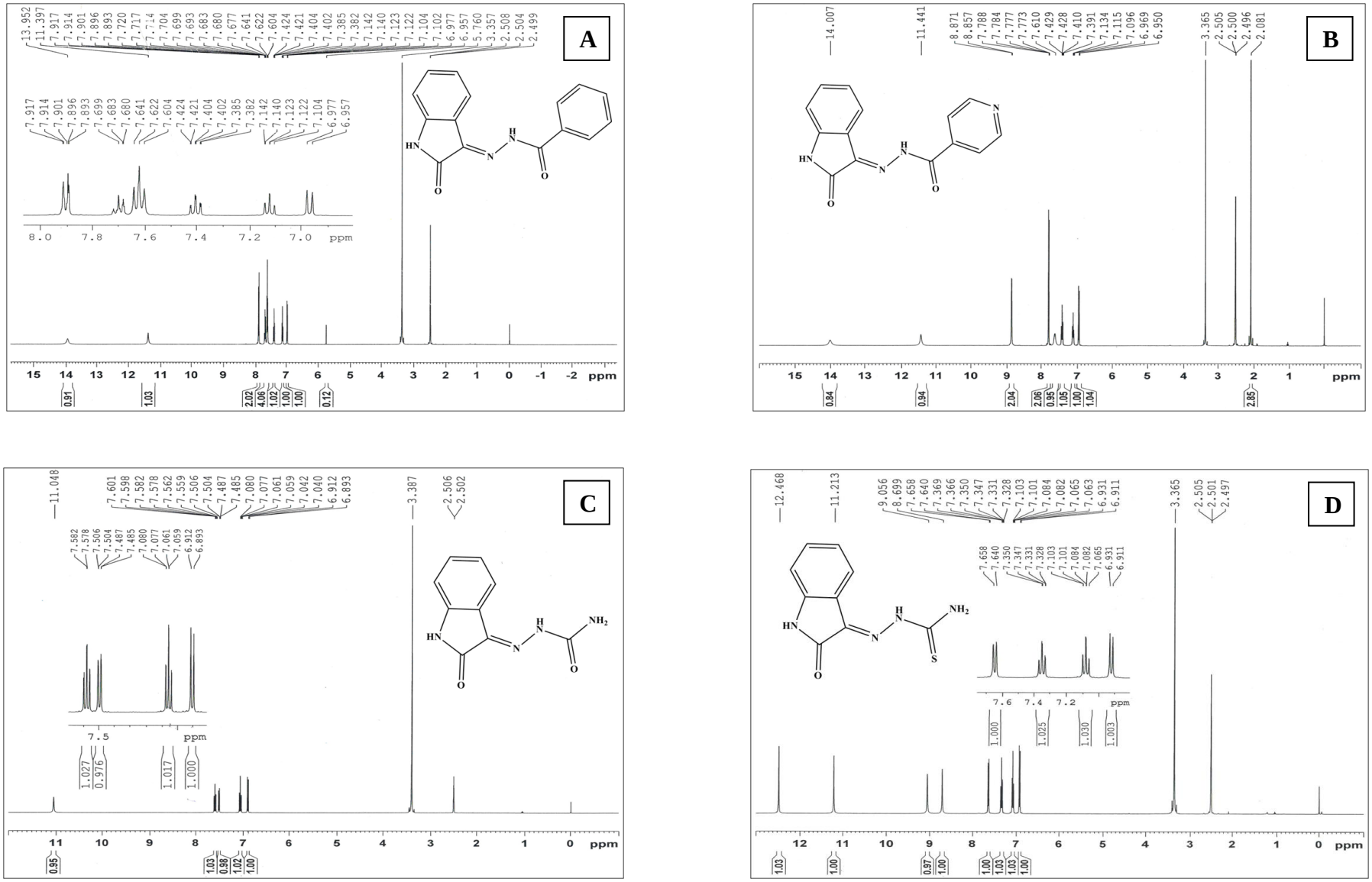

Fig. 2.20: *^{1}H NMR spectra of ligands (A)* ***Isa-1*** *(B)* ***Isa-2*** *(C)* ***Isa-3*** *(D)* ***Isa-4***

2.6 Fluoroquinolones

The fluoroquinolones are a group of synthetic antibiotics that possess broad-spectrum antibacterial activities. After the discovery of the first fluoroquinolone, norfloxacin [73] in 1980, several new members of this family have emerged with enhanced activity against Gram positive and anaerobic bacteria and improved pharmacokinetic profile. These fluoroquinolones work as antibacterials by binding to topoisomerase enzymes (DNA gyrase and Topoismerase IV) inducing permanent double stranded DNA breaks, ultimately resulting in cell death. Much has been learned how molecular modifications of the core quinolone structure affect the antibacterial profile. The structure–activity relationship of quinolones has been the subject of extensive review (*Fig. 2.21*) [74-77]. For most of the current agents, a hydrogen at position 2, a carboxyl group at position 3 and a keto group at position 4 in the bicyclic ring cannot be changed without a significant loss of activity. The fluorine atom at position 6 imparts increased intracellular penetration and enhanced DNA gyrase activity and some efficacy against Gram positive bacteria. It can be considered a breakthrough for the enhanced Gram negative activity, which led to the group of the modern 6-fluoro compounds (or second generation quinolones). The substituent at position 7 greatly influences potency, spectrum and safety. A nitrogen heterocyclic moiety is optimal and piperazine, pyrrolidine and their substituted derivatives have been the most successfully employed side chains as evidenced by the compounds currently on the market.

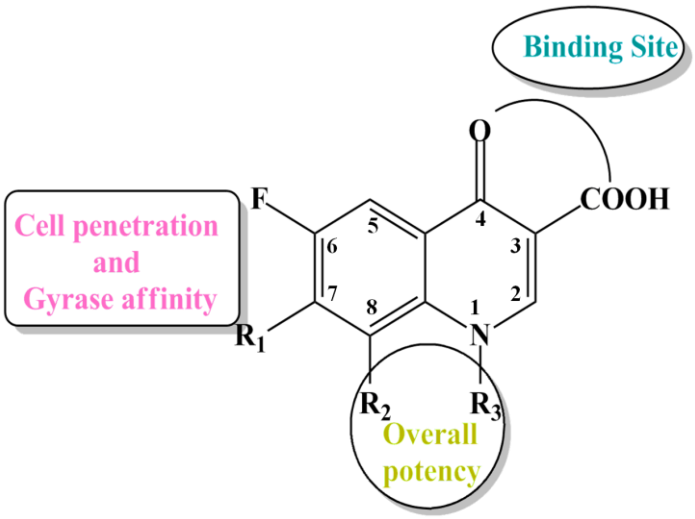

Fig. 2.21: *General structure-activity relationship of the fluoroquinolones.*

These antibiotics are used clinically for the treatment of a wide variety of bacterial infections and a few have been found to be potent enough to cure cancerous tumours also. High oral doses have been reported to reach solid tissues including lung in detectable amounts [78,79]. Some members of this family of compounds have been shown to exert anti-tumor activity in cancer cell lines as well as in animal model. So far, the antitumor activity has been

reported mainly against colon cancer, bladder cancer and leukemia cell lines and has been linked to its topoisomerases II inhibitory activity [80,81]. Ciprofloxacin has a significant anti-proliferative and apoptotic activity on bladder tumor cells [78,82]. Azema *et al.* [83] carried out screening of C-7 modified ciprofloxacin derivatives against prostate (PC-3), glioblastoma (U373-MG), colorectal (LoNo), NSCLC (A549) and breast (MCF7) human cancer cell lines and had reported a superior antitumor activity than the parent ciprofloxacin. Additional target for the antitumor action of quinolones was thought to be the telomerase enzyme, which is noticeably activated in tumor cells [84].

Certain key advantages of fluoroquinolone therapy:

- facile penetration into inflammatory fluids
- attainment of higher concentration in the cell than serum levels
- concentration of fluoroquinolones in the lung reaches around 4-fold higher than serum levels

Looking at the anti-proliferative activity of the fluoroquinolones, we proposed to incorporate this series of ligand into our study. Here we took three different fluoroquinolones: Lemofloxacin (**Flq-1**), Levofloxacin (**Flq-2**) and Ciprofloxacin (**Flq-3**) (*Fig. 2.22*) which were procured as generous gifts from local pharmaceutical companies with 99% HPLC purity.

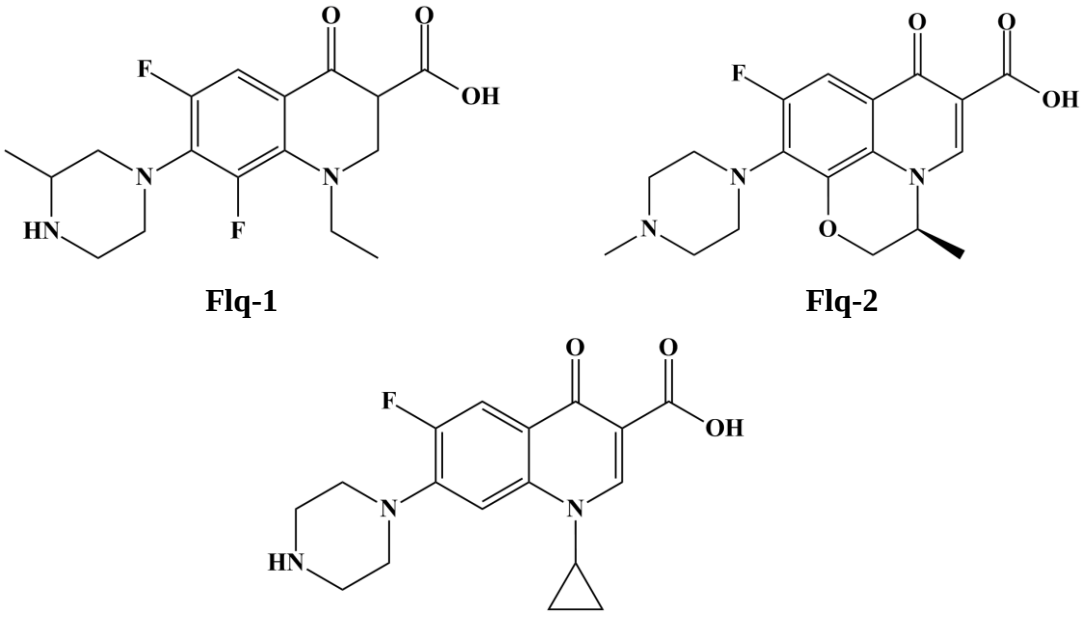

Fig. 2.22: *Structures of the fluoroquinolones employed in the present study.*

2.7 Summary

The five different ligand series discussed in this chapter have been synthesized and well characterized with an aim to employ these organic bioactive ligands in the synthesis of mixed ligand Ru(II) complexes and check their bioactivities.

2.8 References

[1] Chin, Y. W.; Balunas, M. J.; Chai, H. B.; Kinghorn, A. D. *Drug Discovery From Natural Sources. AAPS J.*, **2006**, *8*(2), 239.

[2] Koehn, F. E.; Carter, G. T. *Nat. Rev. Drug Discov.*, **2005**, *4*(3), 206.

[3] Cordell, G. A.; Quinn-Beattie, M. L.; Farnsworth, N. R. *Phytother Res.*, **2001**, *15*(3), 183.

[4] Hughes, E. H.; Shanks, J. V. *Metab. Eng.*, **2002**, *4*(1), 41.

[5] Norman, S. R. *Drug Development Res.*, **2008**, *69*, 15.

[6] Mittal, A. *Sci. Pharm.*, **2009**, *77*, 497.

[7] Nagalakshmi, G. *Indian J. Pharm. Sci.*, **2008**, *70*(1), 49.

[8] Joule, J. A.; Mills, K. *Heterocyclic Chemistry*, 4th Ed., Blackwell Publishing, **2000**, pp: 369.

[9] Nekrasov, D. D. *Chem. Heterocycl. Compd.*, **2001**, *37*(3), 263.

[10] Sperry, J. B.; Wright, D. L. *Curr. Opin. Drug Discovery Dev.*, **2005**, *8*, 723.

[11] Katritzky, A. R. *Chem. Heterocyl. Compd.*, **1992**, *28*(3), 241.

[12] Hankes, L. V. In: *Handbook of vitamins, nutritional, biochemical and clinical aspects. Marcel Dekker:* New York, **1984**; pp.329–377.

[13] Arigon, J.; Bernhart, C.; Bouaboula, M.; Casellas, P.; Combet, R.; Jegham, S.; Hllalret, S.; Fraisse, P. *Nicotinamide derivatives, preparation thereof and therapeutic use thereof.* WO 2009074749A2, **2009**.

[14] Aanandhi, M. V.; Mansoori, M. H.; Shanmugapriya, S.; George, S.; Shanmugasundaram, P. *Res. J. Pharm. Biol. Chem. Sci*,. **2010**, *1*, 1083.

[15] Kheradmand, A.; Navidpour, L.; Shafaroodi, H.; Saeedi-Motahar, G.; Shafiee, A. *Med. Chem. Res.*, **2013**, *22*, 2411.

[16] De Souza, M. V. N.; Fernandes, E. L.; Pais, K. C.; Vasconcelos, T. A.; Wardell, S. M. S. V.; Wardell, J. L. *J. Chem. Res.*, **2006**, *2*, 93.

[17] Gillespie, S. H. *Antimicrob. Agents Ch.*, **2002**, *46*, 267.

[18] de Souza, M. V. N.; Ferreira, M. D.; Pinheiro, A. C. et al *The scientific world journal* **2008**, *8*, 720.

[19] Black, M.; Hussain, H. *Ann. Intern. Med.*, **2000**, *133*, 911.

[20] Kumar, H.; Malhotra, D.; Sharma, R.; Sausville, E.; Malhotra, M. *Pharmacology online*,

2011, *3*, 337.

[21] Rollas, S.; Küçükgüzel, S. *Molecules*, **2007**, *12*, 1910.

[22] (a) Hossein, N.; Khadijeh, R.; Fariba, S. *J. Coord. Chem.*, **2009**, *62*, 1199.

(b) Sakthilatha, D.; Rajavel, R. *J. Chem. Pharm. Res.*, **2013**, *5*, 57.

(c) Hossein, N.; Maryam, N. *J. Chin. Chem. Soc*., **2008**, *55*, 858.

[23] Çakıra, S.; Biçer, E. *J. Iran. Chem. Soc.*, **2010**, *7*, 394.

[24] Gahr, A. A. *Spectrochim. Acta Part A*, **1990**, *46*, 1751.

[25] Sovilj, S. P.; Vasi, V. M.; Stoji, D. L.; Stojeva-Radovanovi, B.; Petkovska, L. T. *Spect. Lett*. **1998**, *31*, 1107.

[26] Christophe, B.; Nadine, F.; Lucien, M.; Jacques, B.; Daniel, P. *Bioorg. Med. Chem. Lett.*, **2000**, *10*, 839.

[27] Epton, R.; Marr, G.; Rogers, G. K. *J. Organomet. Chem.*, **1976**, *110*, 42.

[28] Christophe, B.; Laurence, D.; Lucien, A. M.; Marlène, M.; Daniel, C.; Jacques, S. B. *Eur. J. Med. Chem.*, **2000**, *35*, 707.

[29] Francois, B.; Frederic, C.; Laure, V.; Jacques, B.; Bernard, M.; Anne, R. *J. Med. Chem.*, **2010**, *53*, 4103.

[30] Ion, A.; Moutet, J.; Saint-Aman, E.; Royal, G.; Gautier- Luneau, I.; Bonin, M.; Ziessel, R. *Eur. J. Inorg. Chem.* **2002**, *6*, 1357.

[31] Kuo, L. J.; Liao, J. H.; Chen, C. T.; Huang, C. H.; Chen, C. S.; Fang, J. M. *Org. Lett.* **2003,** *5*, 1821.

[32] Westwood, J.; Coles, S. J.; Collinson, S. R.; Gasser, G.; Greem, S. J.; Hursthouse, M. B.; Light, M. E.; Tucker, J. H. *Organometallics*, **2004**, *23*, 946.

[33] Inouye, M.; Hyodo, Y.; Nakazumi, H. *J. Org. Chem.* **1999**, *64*, 2704.

[34] Takase, M.; Inouye, M. *J. Org. Chem.* **2003**, *68*, 1134.

[35] Debroy, P.; Banerjee, M.; Prasad, M.; Moulik, S. P.; Roy, S. *Org. Lett.* **2005**, *7*, 403.

[36] Seio, K.; Mizuta, M.; Terada, T.; Sekine, M. *J. Org. Chem.* **2005**, *70*, 10311.

[37] Gellett, A. M.; Huber, P. W.; Higgins, P. J. *J. Organomet. Chem.* **2008**, *693*, 2959.

[38] Higgins, P. J.; Gellett, A. M. *Bioorg. Med. Chem. Lett.* **2009**, *19*, 1614.

[39] Top, S.; Vessières, A.; Leclercq, G.; Quivy, J.; Tang, J.; Vaissermann, J.; Huché, M.; Jaouen, G. *Chem. A Eur. J*. **2003**, *9*, 5223.

[40] Jaouen, G.; Top, S.; Vessières, A.; Leclercq, G.; McGlinchey, M. J. *Curr. Med. Chem.* **2004**, *11*, 2505.

[41] Vessières, A.; Top, S.; Pigeon, P.; Hillard, E.; Boubeker, L.; Spera, D.; Jaouen, G. *J. Med. Chem.* **2005**, *48*, 3937.

[42] Hillard, E.; Vessières, A.; Thouin, L.; Jaouen, G.; Amatore, C. *Angew. Chem. Int. Ed.* **2006**, *45*, 285.

[43] Vessieres, A.; Top, S.; Beck, W.; Hillard, E.; Jaouen, G. *Dalton Trans.* **2006**, *4*, 529.

[44] Nguyen, A.; Hillard, E. A.; Vessières, A.; Top, S.; Pigeon, P.; Jaouen, G. *Chimia* **2007**, *61*, 716.

[45] Buriez, O.; Heldt, J. M.; Labbé, E.; Vessières, A.; Jaouen, G.; Amatore, C. *Chem. A Eur. J.* **2008**, *14*, 8195.

[46] Michard, Q.; Jaouen, G.; Vessieres, A.; Bernard, B. A. *J. Inorg. Biochem.* **2008**, *102*, 1980.

[47] Pigeon, P.; Top, S.; Zekri, O.; Hillard, E. A.; Vessières, A.; Jaouen, G. *J. Organomet. Chem.* **2009**, *694*, 895.

[48] Gormen, M.; Plazuk, D.; Pigeon, P.; Hillard, E.; Top, S.; Vessières, A.; Jaouen, G. *Tetrahedron Lett.* **2010**, *51*, 118.

[49] Ornelas, C. *New J. Chem.* **2011**, *35*, 1973.

[50] Prousek, J. *Pure Appl. Chem*. **2007**, *79*, 2325.

[51] Tauchman, J.; Süss-Fink, G.; Stepnicka, P.; Zava, O.; Dyson, P. J. *J. Organomet. Chem.* **2013**, *723*, 233.

[52] Goswami, T. K.; Chakravarthi, B. V. S. K.; Roy, M.; Karande, A. A.; Chakravarty, A.R. *Inorg. Chem.* **2011**, *50*, 8452.

[53] Likhtenshtein, G. *Bioactive Stilbenes, in Stilbenes:* Applications in Chemistry, Life Sciences and Materials Science, Wiley-VCH Verlag GmbH & Co. KGaA, Weinheim, Germany, **2009**

[54] Chong, J.; Poutaraud, A.; Hugueney, P. *Plant Sci.* **2009**, *177*,143.

[55] Mazué, F.; Colin, D.; Gobbo, J.; Wegner, M.; Rescifina, A.; Spatafora, C.; Fasseur, D.; Delmas, D.; Meunier, P.; Tringali, C.; Latruffe, N. *Eur. J. Med. Chem.* **2010**, *45*, 2972.

[56] Li, H.; Wu, W. K. K.; Zheng, Z.; Che, C. T.; Yu, L.; Li, Z. J.; Wu, Y. C.; Cheng, K.-W.; Yu, J.; Cho, C. H.; Wang, M. *Biochem. Pharmacol.* **2009**, *78*, 1224.

[57] Gosslau, A.; Pabbaraja, S.; Knapp, S.; Chen, K. Y. *Eur. J. Pharmacol.* **2008**, *587*, 25.

[58] Quideau, S.; Deffieux, D.; Pouysegu, L. *Angew. Chem. Int. Ed.* **2012**, *51*, 6824.

[59] Fulda, S. *Drug Discovery Today*, **2010**, *15*(17–18), 757.

[60] Patel, K. N.; Kamath, B. V.; Bedekar A. V. *Tet. Lett.* **2013**, *54*, 80.

[61] Petrov O. I.; Gerova, M.; Chanev, Ch.; Petrova, K.V. *Synthesis* **2011**, 3711.

[62] Cella, R.; Stefani, H.A. *Tetrahedron* **2006**, *62*, 5656.

[63] Gaukroger, K.; Hadfield, J. A.; Hepworth, L. A.; Lawrence, N. J.; McGown, A. T. *J. Org. Chem*. **2001**, *66*, 8135.

[64] Myers, A. G.; Tanaka, D.; Mannion, M. R. *J. Am. Chem. Soc.* **2002**, *124*, 11250.

[65] Bellucci, G.; Chiappe, C.; Lo Moro, G. *Tetrahedron Lett.* **1996**, *37*, 4225.

[66] Gerova, M.; Georgieva, S.; Chanev, C.; Petrov, O. I. *Acad. Bulg. Sci.* **2011**, *64*, 1415.

[67] Borrel, C.; Thoret, S.; Cachet, X.; Guernard, D.; Tillequin, F.; Koch, M.; Michel, S. *Bioorg. Med. Chem.* **2005**, *13*, 3853.

[68] Sun, H. Y.; Xiao, C. F.; Cai, Y.-C.; Chen, Y.; Wei, W; Liu, X.-K.; Lv, Z.-L.; Zou, Y. *Chem. Pharm. Bull.* **2010**, *58*, 1492.

[69] Javad, A.; Mohammad, K. M.; Omidreza, F.; Nima, R.; Ramin, M. *Medicinal Chemistry Research.* **2011**.

[70] Charles, M. C. *Thesis- Synthesis of Isatin Derivatives Used for the Inhibition of Pro-Apoptotic Jurkat T Cells.* **2011**.

[71] Gang, C.; Wang, Y.; Xiaojiang, H.; Shuzhen, M.; Qianyun, S. *Chemistry Central Journal.* **2011**.

[72] Soheila, K.; Mohammad, M. K.; Parvaneh.P.; Hadi, A. *Molecular Biology Report*. 2012, 39, 3853.

[73] Koga, H.; Itoh, A.; Murayama, S.; Suzue, S.; Irikura, T. *J. Med. Chem.* **1980**, *23*, 1358.

[74] Wagman, A. S.; Wentland, M. P. *In Comprehensive Medicinal Chemistry II; Taylor, J. B., Triggle, D. J*., Eds.; Elsevier LTD: Oxford, **2007**; Vol. 7, pp 567–596.

[75] Bryskier, A. *In Antimicrobial agents: Antibacterials and Antifungals; Bryskier, A.,* Ed.; ASM Press: Washington, **2005**; pp 668–788.

[76] Dalhoff, A.; Schmitz, F.-J. *Eur. J. Clin. Microbiol. Infect. Dis*., **2003**, *22*, 203.

[77] Peterson, L. R. *Clin. Infect.Dis.* **2001**, *33*, S180.

[78] Herold, C.; Ocker, M.; Ganslmayer, M.; Gerauer, H.; Hahn, E. G.; Schuppan, D. *Br. J. Cancer*, **2002**, *86*, 443.

[79] Sharma, A. K.; Khosla, R.; Kelaand, A. K.; Mehta, V. L. *Indian J Pharmacol.*, **1994**, *26*, 249.

[80] Anderson, V. E.; Osheroff, N. *Curr. Pharm. Des* **2001**, *7*, 337.

[81] Bromberg, K. D.; Burgin, A. B.; Osheroff, N. *Biochemistry*, **2003**, *42*, 3393.

[82] Aranha, O.; Grignon, R.; Fernandes, N.; McDonnell, T. J.; Wood, D. P.; Sarkar, F. H.) *J. Oncol*., **2003**, *22*, 787.

[83] Azema, J.; Guidetti, B.; Dewelle, J.; Le, C. B.; Mijatovic, T.; Korolyov, A.; Vaysse, J.; Malet-Martino, M.; Martino, R.; Kiss, R. *Bioorg. Med. Chem*., **2009**, *17*, 5396.

[84] Yamakuchi, M.; Nakata, M.; Kawahara, K.; Kitajima, I.; Maruyama, I. *Cancer Lett.*, **1997**, *119*, 213.